NEURAL MECHANISMS OF SHORT-TERM VISUAL PLASTICITY AND CORTICAL DISINHIBITION

A Dissertation
Presented to
The Academic Faculty

by

Nathan Allen Parks

In Partial Fulfillment
of the Requirements for the Degree
Doctor of Philosophy in the
School of Psychology

Georgia Institute of Technology
May 2009

NEURAL MECHANISMS OF SHORT-TERM VISUAL PLASTICITY AND CORTICAL DISINHIBITION

Approved by:

Dr. Paul M. Corballis, Ph.D., Advisor
School of Psychology
Georgia Institute of Technology

Dr. Eric H. Schumacher, Ph.D.
School of Psychology
Georgia Institute of Technology

Dr. Randall W. Engle, Ph.D.
School of Psychology
Georgia Institute of Technology

Dr. Daniel H. Spieler, Ph.D.
School of Psychology
Georgia Institute of Technology

Dr. Krish Sathian, M.D., Ph.D.
Department of Neurology
Emory University School of Medicine

Date Approved: April 1, 2009

ACKNOWLEDGEMENTS

I wish to thank my advisor, Paul Corballis, for his guidance, patience, and friendship all these years. Without his mentorship I could never have made it this far. I would also like to thank my dissertation committee members Randy Engle, Krish Sathian, Eric Schumacher, and Dan Spieler for their insightful comments and input. My family, Allen, Leah, Tessa, and Josh Parks have always been a major source of inspiration and support. I cannot thank them enough. Most of all, I must express an incredible degree gratitude to my wife, Nadya, has been extremely patient and supportive over the years and particularly so these past few stressful months!

TABLE OF CONTENTS

LIST OF FIGURES

SUMMARY

Deafferented cortical visual areas exhibit topographical plasticity such that their constituent neural populations adapt to the loss of sensory input through the expansion and eventual remapping of receptive fields to new regions of space. Such representational plasticity is most compelling in the long-term (months or years) but begins within seconds of retinal deafferentation (short-term plasticity). The neural mechanism proposed to underlie topographical plasticity is one of disinhibition whereby long-range horizontal inputs are "unmasked" by a reduction in local inhibitory drive. In this dissertation, four experiments investigated the neural mechanisms of short-term visual plasticity and disinhibition in humans using a combination of psychophysics and event-related potentials (ERPs). Short-term visual plasticity was induced using a stimulus-induced analog of retinal deafferentation known as an artifical scotoma. Artificial scotomas provide a useful paradigm for the study of short-term plasticity as they induce disinhibition but are temporary and reversible. Experiment 1 measured contrast response functions from within the boundaries of an artificial scotoma and evaluated them relative to a sham control condition. Changes in the contrast response function suggest that disinhibition can be conceived of in terms of two dependent but separable processes: receptive field expansion and unrestricted neural gain. A two-process model of disinhibition is proposed. A complementary ERP study (Experiment 2) recorded visual evoked potentials elicited by probes appearing within the boundaries of an artificial scotoma. Results revealed a neural correlate of disinhibition consistent with origins in striate and extrastriate visual areas. Experiment 3 and 4 were exploratory

examinations of the representation of space surrounding an artificial scotoma and revealed a neural correlate of invading activity from normal cortex. Together, the results of these four studies strengthen the understanding of the neural mechanisms that underlie short-term plasticity and provide a conceptual framework for their evaluation.

CHAPTER 1

INTRODUCTION

Primary sensory areas in mammalian cortex are organized topographically (Felleman, Wall, Cusick, & Kaas, 1983; Real & Imig, 1980; Tootell, Switkes, Silverman, & Hamilton, 1988; Tusa, Palmer, & Rosenquist, 1978). It was long held that the topography of sensory areas was modifiable only during critical periods of development and could be considered 'hard-wired' thereafter (Hubel & Wiesel, 1970). Research conducted over the past two decades has shown that, in fact, sensory cortices exhibit a remarkable degree of plasticity and are capable of topographic reorganization even in adulthood.

The first compelling evidence of cortical topographic plasticity came from studies of somatosensory cortex. Following digit amputation, the topographical organization of primary somatosensory cortex underwent a dramatic alteration such that the region of cortex that had previously represented the amputated digit became responsive to the stimulation of adjacent digits (Merzenich, 1983a, 1983b, 1984; Rasmusson, 1982). Further investigation revealed that not only did somatosensory cortex reorganize after several months but the beginning of such reorganization was measurable within minutes of digit amputation (Calford & Tweedale, 1988, 1991a, 1991b). These studies prompted investigations of plasticity in other sensory modalities and it was soon apparent that topographical reorganization was not restricted to somatosensory cortex but also occurred in auditory (Rajan, Irvine, Wise, & Heil, 1993; Robertson & Irvine, 1989), motor (Sanes, Suner, & Donoghue, 1988), and visual (Kaas et al., 1990) cortices. The primary concern

of this dissertation is plasticity within the visual system and discussion will focus on this modality (see Calford, 2002 for review of reorganization in other modalities).

As with somatosensory cortex, large-scale topographic reorganization occurs within primary visual cortex following deafferentation. Using lasers to induce small retinal lesions a number of single-cell studies have found extensive reorganization within V1 (Gilbert & Wiesel, 1992; Heinen & Skavenski, 1991; Kaas, Krubitzer, Chino, Langston, Polley, & Blair, 1990). In general these studies have found that after several months of recovery deafferented regions of cortex became reactive and remapped their classical receptive fields to new regions of space. Changes in receptive fields (RFs) also occur within minutes of lesioning. However, such short-term plasticity results in RF expansions rather than absolute remapping of visual space (Calford, Schmid, & Rosa, 1999; Calford, Wang, Taglianetti, Waleszcyk, Burke, & Dreher, 2000; Gilbert & Wiesel, 1992).

Very little research has examined adult topographical plasticity within human visual cortices. Long-term visual plasticity has been examined using functional imaging in patients with abnormal visual input (Baker, Peli, Knouf, & Kanwisher, 2005; Dilks, Serences, Rosenau, Yantis, & McCloskey, 2007). These studies are consistent with the occurrence of large-scale visual reorganization reported in single-cell unit studies conducted in animals. However, short-term visual plasticity in humans remains unexplored. In this dissertation, I examine neural correlates of short-term visual plasticity in humans using psychophysical measures and event-related potentials (ERPs).

Lesioning methods are impractical for the empirical investigation of short-term plasticity and cannot be used in human subjects. However, a temporary and reversible

stimulus-induced analog of retinal deafferentation known as an artificial scotoma (Ramachandran & Gregory, 1991) can be used to investigate short-term visual plasticity in humans. Artificial scotomas provide an effective method of assessing short-term visual plasticity since induce the same change in receptive field properties as a true lesion (De Weerd & Pessoa, 2003; De Weerd, Gattass, Desimone, & Ungerleider, 1995; Pettet & Gilbert, 1992) but can be used routinely without harm to the subject.

Four experiments investigated disinhibition and short-term plasticity in the human visual system using an artificial scotoma paradigm. Experiments 1 and 2 examined plasticity induced within the region of cortex temporarily deafferented by an artificial scotoma (i.e., within the boundaries of the artificial scotoma). Experiment 1 was concerned with evaluating changes in receptive field dynamics within deafferented visual cortex using psychophysical measurement of contrast response functions. Specifically, three models of receptive field dynamics were contrasted. Experiment 2 employed event-related potentials (ERPs) to identify neural correlates of short-term plasticity and to determine the earliest level within the human visual hierarchy at which these short-term plastic changes can be found.

Experiments 3 and 4 were exploratory examinations that investigated plasticity-induced perceptual and electrophysiological changes in the region of space surrounding the artificial scotoma. Plasticity within deafferented cortex is partly the result of horizontal inputs originating from surrounding cortex. As such, an increase in the neural representation of extra-scotoma space may be expected due to this invading activity and may alter cortical visual processing within surrounding cortex. Experiment 3

investigated the perceptual consequences of invading activity whereas Experiment 4 sought a neural correlate of the process using ERP.

Plasticity: Definition & Related Terms

The word *plasticity* is a rather overused term in the neuroscience vernacular. In general, plasticity refers to some neural change that accompanies learning, experience, sensory deafferentation, or brain damage. However, such a definition is exceedingly broad and it is necessary to clarify the meaning of the term as it will be used in this document. From hereon, the term *plasticity* will refer to *representational (topographical) plasticity*, meaning that there has been a change in some aspect of cortical topography. Before specifying further what is meant by representational plasticity several other terms must first be introduced. The term *classical receptive field* refers to the region of space to which the cell is responsive under conditions of normal visual input and when mapped with stimuli presented on a uniform background. When used in the context of receptive fields, the qualifiers *remapped* or *shifted* refer to a region of space other than the classical RF to which a cell has become responsive. These two terms will imply that, relative to the classical receptive field, RF size remains approximately unchanged. The term *ectopic* is used to generally describe a receptive field that has been spatially altered in some way from the classical receptive field. This could imply that the RF has shifted or remapped, or could mean that the RF has increased in area or shape. The terms *expanded RF* and *RF expansion* are used to specifically describe RFs that are of considerably greater area than the classical RF. The term *deafferented zone (DZ)* will refer to a region of cortex

deprived of visual sensory input (deafferented). *DZ* will describe a permanent deafferentation of sensory cortex due to retinal lesion. A complementary term, *temporary deafferented zone (TDZ)*, will refer to a region of cortex temporarily deprived of patterned visual input by means of a stimulus-induced artificial scotoma. *Invading zone (IZ),* refers to the cortical area surrounding a DZ or TDZ that provides long-range horizontal inputs to that area. DZ, TDZ, and IZ will be used generally to refer to those cortical visual areas that experience a loss of sensory input from visual space. When necessary to describe specific cortical areas, the terms will qualified with the appropriate label. For example, V1-DZ refers to the deafferented region of primary visual cortex. With the aforementioned terms defined, a more precise definition of plasticity can be given. *Representational plasticity, topographical plasticity,* and *plasticity* will refer simply to the systematic occurrence of ectopic RFs within a DZ or TDZ. This means that RFs have remapped, changed in size, or changed in shape. With respect to the time course of plasticity the terms *reorganization* and *long-term plasticity* will refer to representation plasticity over a course of days, months, or years. *Short-term plasticity* will refer to the occurrence of representational plasticity over seconds, minutes, or hours.

Long-Term Visual Plasticity and Reorganization

It has long been known that the visual cortices are capable of representational plasticity during development but it was thought that this plasticity was restricted to early periods in development and that the response properties of visual cortical neurons were "hard-wired" in adulthood (Hubel & Wiesel, 1970). However, this view has changed a

great deal and it is now widely accepted that even adult visual cortex is capable of considerable reorganization (for reviews see Calford, 2002; Gilbert, 1998).

The first foray into visual topographic plasticity was undertaken in the primary visual cortex (area V1) of adult cats. Following extensive mapping of receptive fields in V1, Kaas and colleagues (1990) used a laser to induce 5-10° monocular lesions in the peripheral retinal of cats. The nonlesioned eye was then enucleated to remove visual input from the partner eye. Two to six months later recordings were again made in V1. Outside the DZ, neurons had receptive fields of both normal size and normal location. However, receptive fields within the DZ were ectopic and represented regions beyond the lesioned retinal area. Thus, the topographical representation of the DZ had reorganized such that classical receptive fields had remapped to new locations.

The general findings of long-term reorganization of V1 have been replicated by a number of single-cell studies in several species (Calford et al., 1999; Gilbert & Wiesel, 1992; Heinen & Skavenski, 1991). However, a recent study has raised some controversy regarding the occurrence and extent of reorganization within primary visual cortex (Smirnakis et al., 2005). Smirnakis and colleagues induced matched binocular lesions in macaque retina and used fMRI to track visual reorganization over a period of seven months. Contrary to previous findings, their results indicated that the DZ within V1 remained silenced months after deafferentation. This result suggested that no reorganization had occurred in V1. The reason for this incongruence with two decades of previous findings is unknown but may be related to differences in measurements of reorganization. Calford and colleagues (2005) suggest that the apparent lack of reorganization described by Smirnakis is merely a reflection of fMRI's (i.e., BOLD)

insensitivity to spiking activity. They argue that spiking activity is the critical dependent measure and the BOLD response is insensitive to changes in spiking activity. It is also unclear how extended periods of deafferentation affect neurovascular coupling. Furthermore, the BOLD response reflects both inhibitory and excitatory neural activity. Deafferentation has been shown to decrease inhibitory GABAergic activity within the DZ (Jones, 1990; Rosier et al., 1995). Thus, it is possible that the lack of BOLD response found within the DZ (i.e., Smirnakis et al., 2005) may be due to the reduction in inhibitory activity even though excitatory activity may actually be increased. Further investigation of these issues is required.

Despite some recent controversy, long-term visual reorganization has been repeatedly demonstrated in cats and monkeys. Evidence of visual plasticity in humans, however, is quite limited. Studies of clinical patients with retinal abnormalities suggest that the human visual cortex may also be capable of reorganization in adulthood. Some of this evidence comes simply from patient self-report. Retinal lesions do not present as "black holes" in visual space, but are 'filled-in' by the space that surrounds them (Morgan & Shatz, 1985; Smith, Lea, & Galloway, 1990; Zur & Ullman, 2003). Peripheral retinal lesions often go unnoticed by patients until explicitly tested (Dreher, Burke, & Calford, 2001). Even patients with central retinal lesions do not perceive a blind spot but rather report that objects and space appear distorted around the lesioned retinal area – a condition known as metamorphopsia (Morgan & Shatz, 1985; Smith et al., 1990). Such perceptual filling-in of visual space is not, in itself, direct evidence of cortical reorganization but is likely to be a perceptual consequence of the process.

More concrete evidence for visual reorganization in humans has come from functional imaging studies of patients with chronic retinal abnormalities such as macular degeneration (MD). Patients with MD have severe degeneration of macular tissue which results in a loss of central vision. MD patients typically compensate for their visual impairment by fixating objects with a new peripheral portion of the retina known as the preferred retinal location (PRL; Timberlake, Mainster, Peli, Augliere, Essock, & Arend, 1986). Baker and colleagues (2005) used fMRI to investigate how normal human retinotopy was altered by the loss of central vision and increased reliance upon a PRL. Specifically, they investigated whether cortex that had once received normal foveal input would reorganize to represent the PRL. Normally, the cortical representation of fovea is located in the most posterior portion of occipital cortex near the occipital pole (the foveal confluence; Dougherty, Koch, Brewer, Fischer, Modersitzki, & Wandell, 2003). Baker and colleagues compared activation of the foveal confluence in normal subjects to that of two patients with MD. Foveal stimulation showed no activation of the foveal confluence in MD patients (due to retinal degeneration). However, photic stimulation of the PRL did activate the foveal confluence. These findings suggest that the central visual deprivation of MD patients had resulted in a large-scale reorganization of visual topography such that foveal representations within the visual cortices had remapped to represent peripheral locations.

Several recent imaging studies of MD patients have replicated the findings of cortical reorganization of the foveal confluence (Baker, Dilks, Peli, & Kanwisher, 2009; Schumacher et al., 2008). Further investigations have suggested that cortical reorganization in these patients is not specific to the PRL, a result which implies that the

reorganization is not necessarily due to a use-dependent mechanisms (Dilks, Baker, Peli, & Kanwisher, 2009; however, see Masuda, Dumoulin, Nakadomari, & Wandell, 2008).

Another study of visual reorganization in an MD patient failed to show any evidence of cortical reorganization (Sunness, Liu, & Yantis, 2004). Sunness and colleagues performed retinotopic mapping in a single patient with macular degeneration. Cortical areas were properly delineated but revealed a consistently silenced region of cortex that corresponded to the patient's scotoma. This finding suggested a lack of reorganization. The reason for the discrepant findings of Sunness and colleagues is unclear. However, one possible explanation is that the MD patient they examined had a spared region of fovea that may act to maintain the spatial representation of central vision to be maintained within the foveal confluence.

Dilks and colleagues (2007) have provided further indication of cortical reorganization in humans. Their evidence comes from a case study of a stroke patient, B.L., whose stroke resulted in selective damage of the inferior portion of the optic radiations in the right hemisphere. The damage suffered by B.L. rendered him blind in a single visual quadrant – the upper left visual field. Dilks and colleagues examined whether deafferentation resulted in cortical reorganization of V1. One indication of reorganization was the fact that B.L. exhibited significant distortions of visual space for stimuli presented in the lower left visual field. Stimuli here appeared elongated, as if extending toward the upper visual field. Such a perceptual distortion may reflect visual reorganization. Further evidence of reorganization came from retinotopic mapping with fMRI. Stimulation of the lower left visual field revealed activations in regions of right V1 that normally represent upper left visual field. That is, photic stimulation of intact

retina induced BOLD activation in deafferented cortex. No such changes were found in B.L.'s left hemisphere which still received input from the entire right side of space. These results are consistent with the occurrence of large-scale visual reorganization.

Short-Term Visual Plasticity

The studies reviewed above were concerned with reorganization weeks, months, or years after sensory deafferentation. However, these studies do not address questions regarding the time course of reorganization. Delineating the time course of representational plasticity is a critical step in understanding the neural mechanisms that underlie representational plasticity in adult sensory cortex. Single-cell studies of sensory cortices indicate that extensive receptive field changes occur in considerably less time than weeks or months but can begin within minutes of deafferentation.

Gilbert and Wiesel (1992) induced matched binocular lesions in cats and macaques and mapped changes in RFs immediately following the lesion and up to three months thereafter. Directly following lesioning, RFs within the center of the DZ were silenced. However, RFs closer to the boundaries of the scotoma expanded up to 10-fold their normal size and were responsive to regions of space beyond their classical RFs. Three months after the lesion, RFs had remapped over even greater distances and constricted to dimensions similar to their classical sizes. Similar findings of short-term receptive field expansions in the DZ have been reported by a number of other studies using matched binocular lesions (Heinen & Skavenski, 1991; Darian-Smith & Gilbert, 1995).

Another strategy for studying short-term visual plasticity has been to induce a single monocular lesion while leaving the partner eye intact to serve as a control (Calford, Schmid, & Rosa, 1999; Chino, Kaas, & Smith, 1992; Schmid, Rosa, & Calford, 1995). Schmid, Rosa, and Calford (1995) used a low-power argon laser to carefully detach a small portion of retina from a single eye in cats. Recordings made within the DZ one to two hours later revealed that RFs expanded and were responsive to regions of the intact portion of retina. However, when stimulated through the intact eye these same neurons revealed receptive fields of normal shape and size. A related study was undertaken by Calford, Schmid, and Rosa (1999). They induced monocular retinal lesions in cat with an argon laser and tracked RF changes up to 11 hours after the lesion. Throughout the course of mapping RFs within the DZ were of normal size and position when stimulated through the intact eye. However, DZ receptive fields were responsive to intact retinal areas when stimulated through the lesioned eye. These changes began within an hour of lesioning and 11 hours later 56% of recorded cells exhibited such ectopic RFs (see also Chino et al., 1992).

Neural Substrates of Visual Reorganization

The studies reviewed above demonstrate that extensive reorganization occurs within primary visual cortex following a retinal lesion and such plasticity begins within seconds to minutes of deafferentation. However, the occurrence of representational plasticity within V1 does not necessarily imply that reorganization begins there. The visual system is organized in a hierarchical fashion and it is possible that reorganization begins at a level even lower than V1.

The earliest possible source of reorganization within the visual system is at the retinal level. Several groups have suggested that lateral interactions mediated by retinal amacrine cells may be able to account for the ectopic RFs measured in primary visual cortex (for review see Dreher et al., 2001). Many laser lesioning procedures destroy the photoreceptor layer of the retina but leave retinal ganglion cells intact. This leaves the possibility that these unharmed ganglion cells receive lateral activation from beyond the lesioned area and continue to provide input into the V1-DZ. However, a retinal level explanation of reorganization is unlikely. First, the RFs of ganglion cells remain unchanged even after V1 reorganization has occurred (Gilbert & Wiesel, 1992). Second, a portion of retina that has been detached from the optic nerve fails to induce any activity in the V1-DZ even though lateral connections continue to function (Schmid et al., 1995). Further evidence against retinal-level reorganization is the lack of reorganization seen in the major target of retinal afferents – the lateral geniculate nucleus (LGN).

Anatomically, the LGN is unlikely to be the source of reorganization since the lateral spread of thalamic afferents is insufficient to account for the extent of reorganization seen in V1. Thalamic afferents from the LGN spread laterally 1.5 – 2.0 mm in layer IV of primary visual cortex (Blasdel & Lund, 1983) but reorganization in V1 typically spans over areas of 6 mm and greater (Darian-Smith & Gilbert, 1995). The growth of new thalamocortical projections is also unable to account for reorganization since V1 plasticity occurs within time periods too short to be attributable to axonal growth and even months after retinal lesioning retrograde neural tracing from V1 reveals no change in the lateral spread of geniculocortical afferents (Darian-Smith & Gilbert, 1995).

The anatomical limitations of geniculocortical input suggest that the LGN is unlikely to account for V1 reorganization. However, if reorganization occurred within the LGN itself these changes could be reflected in V1 as well. Limited LGN reorganization may occur over extended periods of time (Eysel, 1989) but is insufficient to account for the extent of reorganization found within V1. A major source of evidence against LGN-level plasticity is the fact that retinotopically-matched portions of the LGN remain silent even after reorganization has occurred within V1 (Darian-Smith & Gilbert, 1995; Gilbert & Wiesel, 1992). Studies of stimulus-induced artificial scotomas have provided further evidence that V1 plasticity is cortically mediated.

Neither changes within the retina nor the LGN can account for cortical-level reorganization. Thus, the primary visual cortex is the earliest locus to exhibit substantial visual plasticity. Representational plasticity within V1 is thought to be mediated by long-range horizontal projects (Gilbert et al., 1996). Horizontal connections are local pyramidal projections that connect cells with non-overlapping receptive fields over distances of 6-8 mm (Gilbert et al., 1996; Hubel & Wiesel, 1974) making them excellent candidates for mediating cortical reorganization. Furthermore, the lateral spread of horizontal connections approximates the extent over which cortical reorganization is typically reported (Gilbert et al., 1996).

Calford, Wright, Metha, and Taglianetti (2003) confirmed that topographic reorganization within V1 is subserved by long-range horizontal connections using a locally injected neurotoxin. Monocular lesions were placed in the retina of adult cats and considerable V1 reorganization was found several weeks later. Following this period, stimulation via the lesioned eye revealed that RFs within the DZ had remapped. The

contribution of long-range horizontal connections in the formation of these ectopic RFs was examined by injecting kainic acid (an excitatory neurotoxin) into an adjacent area of cortex outside of the DZ (i.e., normal cortex). If V1 reorganization were mediated through long-range horizontal connections then regions of cortex adjacent to the DZ (the IZ) should provide the input necessary for RF remapping to develop. Chemical inactivation of the IZ should then abolish horizontal input and extinguish ectopic RFs. Indeed, when surrounding normal cortex was deactivated with kainic acid, neurons within the DZ were unresponsive to the presentation of photic stimuli in their remapped RF. That is, DZ neurons were silenced by a loss of corticocortical input, a result consistent with the idea that horizontal projections subserve reorganization.

Under normal circumstances horizontal projections provide only subthreshold input to pyramidal cells (Das & Gilbert, 1995a). However, deafferentation is thought to induce changes in the efficiency of horizontal connections – transforming subthreshold input into suprathreshold activity. Das and Gilbert (1995a) used a cortical point-spread (PS) paradigm to delineate the extent over which horizontal activity propagated in normal and reorganized V1 of adult cats. In a point-spread paradigm, the lateral spread of V1 activity is measured by flashing a small photic stimulus (a point) at a desired retinotopic position. Single-cell recordings were used in conjunction with voltage-sensitive optical imaging to determine how subthreshold and suprathreshold activity changed following V1 reorganization. Single-cell recordings (spiking PS) are sensitive to suprathreshold spiking activity whereas optical imaging (optical PS) measures to both subthreshold and suprathreshold activity. The combination of these two methods allowed changes in horizontal synaptic efficiency to be examined. In normal adult cats, optical imaging

revealed subthreshold activity over a cortical area of 4 mm whereas suprathreshold spiking activity was confined to the central 5% of this region (~750 µm). Reorganized V1 revealed quite a different point-spread pattern. After several months of V1 reorganization, a shift in activity was seen in the DZ such that spiking PS extended over an area of 4 mm. Note that this suprathreshold area in the DZ was equivalent to the subthreshold optical PS in normal adult cats. Thus, previously subthreshold horizontal inputs became suprathreshold following cortical reorganization.

Long-range horizontal connections provide an anatomical basis for cortical reorganization but their existence does not completely describe the neural mechanism through which such plasticity occurs. It is thought that representational plasticity is the result of an unmasking of subthreshold horizontal inputs due to decreased inhibitory activity – a process termed *disinhibition*. Classical receptive fields are formed from a balance of excitatory and inhibitory input and RF structure can be modeled to a reasonable extent as an excitatory center region with an inhibitory surround (Sceniak, Ringach, Hawken, & Shapely, 1999). The major excitatory input of an RF comes mainly from thalamocortical afferents whereas inhibition is a result of input from local GABAergic interneurons (Tremere et al., 2005). Inhibitory GABAergic interneurons are a critical determinant of receptive field size and stimulus selectivity (e.g., directional preference). The blockade of inhibitory GABAergic activity has been shown to dramatically alter the properties of classical RFs. Ionotophoretic infusion of bicuculline methiodide (BMI), a competitive GABA antagonist, results in RF expansion and a loss of orientation and directional selectivity (Sillito, 1975; Wolf, Hicks, & Albus, 1983). That

is, without inhibitory input from interneurons, RFs enlarge and respond nonselectively to stimuli within the enlarged RF.

Long-range horizontal connections in V1 provide subthreshold excitatory inputs to other pyramidal cells yet stimulation of RF surrounds typically has inhibitory effects on RF centers. This seemingly paradoxical finding is attributable to that fact that horizontal connections do not provide input solely to pyramidal cells but also provide excitatory input to GABAergic interneurons (McGuire, Gilbert, Rivlin, & Wiesel, 1991). Thus, horizontal activity will excite both pyramidal cells and inhibitory GABAergic interneurons resulting in a net effect of inhibition in the RF surround.

Excitatory horizontal input to pyramidal cells is normally kept in check by local GABAergic inhibition. However, the removal of inhibitory GABAergic activity allows previously subthreshold excitatory horizontal connections to exert greater influence over pyramidal cells. Reconsider the results from BMI ionotophoresis in this framework of disinhibition. Local infusion of BMI around a pyramidal cell removes inhibitory influences on the cell. This disinhibition increases the weighting of inputs from excitatory long-range horizontal connections. With local inhibition removed, non-overlapping spatial information from neurons up to 8 mm away is now capable of influencing the neuron's activity. This expansive input increases the representation of space from which a cell receives information.

In the case of BMI infusion, disinhibition is induced artificially. However, disinhibition in primary visual cortex also occurs under natural conditions as well. Following long-term retinal deafferentation GABAergic activity and receptor synthesis within the DZ are significantly down-regulated (Benson, Huntsman, & Jones, 1994;

Jones, 1990; Rosier et al., 1995). Disinhibition is also found following short-term deafferentation (Das & Gilbert, 1995; De Weerd, Gattass, Desimone, & Ungerleider, 1995; Pettet & Gilbert, 1992; Tremere et al., 2003, 2005). In this case, disinhibition results from activity-dependent reductions in inhibitory drive within the DZ (Tremere et al., 2003, 2005).

Disinhibition is widely held as the mechanism of long-term reorganization and short-term plasticity. However, it should be noted that feedback connections from higher-order visual areas may also play a role. Later visual areas are well known to have larger RFs and feedback from these later visual areas could influence representational plasticity, particularly over the short-term. This possibility has not yet been systematically investigated but some evidence suggests that local horizontal projections, rather than feedback connections, are the primary source of plasticity (Gilbert, 1998).

Short-Term Visual Plasticity: Artificial Scotomas

It is clear from animal studies that visual reorganization begins within minutes of deafferentation (e.g., Gilbert & Wiesel, 1992). The study of plasticity over short time scales is theoretically important as short-term changes are likely to provide insight into the neural mechanisms underlying plasticity. The study of long-term cortical reorganization has prompted many further questions regarding the mechanism and time course of plasticity. How do RF properties change directly following deafferentation? What happens to receptive field structures within seconds of a lesion? Do receptive fields begin to expand and remap immediately, or does the process take time? These questions are not easily answered using lesioning techniques. Technical limitations and

side effects of the lesioning procedure preclude the use of this methodology to examine short-term visual plasticity (Dreher et al., 2001).

Evidence of short-term visual plasticity following a retinal lesion is nonexistent in humans. Studies of visual plasticity in humans have relied upon functional imaging of small patient populations whom already exhibit long-term reorganization. The study of these patients is conducive only to the study of long-term plasticity and new methods must be employed to properly study short-term plasticity in humans.

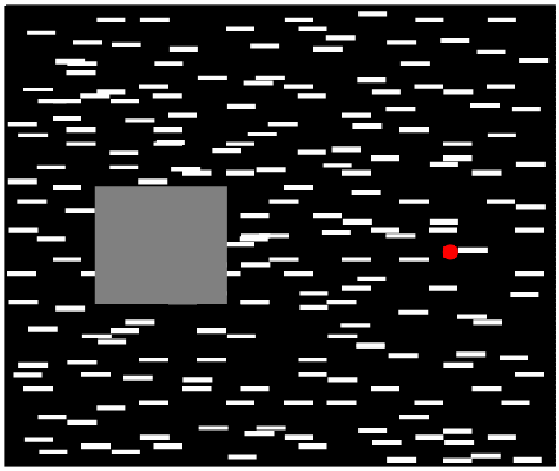

Figure 1. A single frame from a typical artificial scotoma paradigm. The red dot is the fixation point. The white bars form the dynamic background and randomly shift position many times per second. The gray box represents the scotoma area that appears to become filled-in by the dynamic background. The perceptual filling-in of an artificial scotoma can, in fact, occur in the absence of motion. If fixation is steadily maintained on the red dot above, the gray box will eventually fade from view. Filling-in of the illusion is expedited by the introduction of motion to the background stimulus.

One such method of examining the short-term effects of plasticity is that of an artificial scotoma. An artificial scotoma is a stimulus-induced method of mimicking sensory deafferentation by restricting patterned visual input from a small region of space. In an artificial scotoma paradigm an observer maintains fixation in the presence of a

dynamically fluctuating background superimposed upon which is a static and uniform area (Figure 1). When exposed to such a display for several seconds the box appears to fade from perception and becomes filled-in by the dynamic texture that surrounds it (De Weerd, Desimone, & Ungerleider, 1998; De Weerd, Smith, & Greenburg, 2006; Ramachandran & Gregory, 1991). With accurate fixation an artificial scotoma restricts visual input from a region of space and temporarily deafferents the retinotopically-matched region of visual cortex, thus resulting in a TDZ.

Several single-cell studies have demonstrated that, like a true retinal lesion, an artificial scotoma, induces short-term plasticity within the TDZ (Gilbert & Weisel, 1992; Pettet & Gilbert, 1992). However, unlike a true retinal lesion, the short-term plasticity of an artificial scotoma can be reversed through simple visual stimulation (Gilbert & Weisel, 1992). The neural mechanisms underlying the short-term plasticity of an artificial scotoma appear to be identical to those following a true retinal lesion (i.e., disinhibition; De Weerd & Pessoa, 2003). The artificial scotoma paradigm provides a practical model for the study of short-term plasticity as it induces the same short-term changes in receptive field dynamics and allows for repeated testing and measurement from a TDZ.

The generally accepted neural mechanism of short-term visual plasticity is that of disinhibition. However, results from single-cell studies have suggested several different proposals regarding the functional consequences of disinhibition on receptive field dynamics. One proposal has been that disinhibition induces receptive field expansions (*RF expansion*; Das & Gilbert, 1995b; Pettet & Gilbert, 1992; Volchan & Gilbert, 1995). Pettet and Gilbert (1992) examined short-term plastic changes accompanying an artificial

scotoma in V1 of anesthetized adult cats. Artificial scotomas were conditioned for approximately ten minutes and receptive field size was quantified for neurons within the TDZ. They reported an average five-fold expansion relative to a cell's classical receptive field. Das and Gilbert (1995) used a cross-correlation technique to investigate RF expansions in anesthetized adult cats. The spiking activity between pairs of neurons separated by up to 5 mm was cross correlated when these RFs fell within an artificial scotoma. Cross-correlation between neuron pairs increased significantly when RFs fell within the boundaries of an artificial scotoma, indicative of RF expansion. A psychophysical study in humans also supports the proposal of receptive field expansion. Kapadia, Gilbert, and Westheimer (1994) demonstrated perceptual spatial distortions following the conditioning of an artificial scotoma. Within the boundaries of the scotoma psychophysical acuity thresholds demonstrated that the perception of space was "compressed" toward the scotoma's center, a result is consistent with RF expansions.

A second account regarding the effects of disinhibition due to an artificial scotoma suggests that receptive field size remains unaltered but it is the cell's neural response gain that changes, increasing in firing rate (*RF gain*). DeAngelis and colleagues (1995) conducted a study similar to that of Pettet and Gilbert (1992) but found no evidence of receptive field expansions. Instead, their results suggested that TDZ neurons exhibited a multiplicative increase in response to stimuli within their RF but had no change in the size or shape of RFs. Their data suggested that increased gain had occurred without affecting the response selectivity of cells. Though the effect of gain was clearly demonstrated, inferences regarding the selectivity of neural response were drawn from

one-dimensional receptive field profiles which render it difficult to interpret how selectivity (e.g., orientation-tuning) was affected.

A different account of short-term plasticity was offered by De Weerd and colleagues (1995). Using single-cell recordings in awake monkeys they described plastic changes resulting from conditioning with an artificial scotoma that they termed 'climbing activity.' Recordings were made from cells that had RFs within the boundaries of an artificial scotoma. Initial recordings revealed little change in spiking activity relative to baseline. However, over several seconds of conditioning with an artificial scotoma spiking activity gradually ramped-up to a level that matched neural responses to the dynamic texture alone. No evidence of RF expansion was found before, during, or after scotoma conditioning and results were interpreted as a correlate of perceptual filling-in rather than RF expansion. This climbing activity is consistent with both receptive field expansion and neural response gain. The effect of climbing activity was a linear increase in response gain (firing rate) as a function of time. However, climbing activity could also be interpreted to reflect RF expansion. That is, it could be the case that the cell's RF gradually expanded over several seconds and became more and more responsive to regions of space beyond the classical receptive field (outside scotoma boundaries). Photic stimulation within an expanded RF causes a rapid collapse back to the CRF (Pettet & Gilbert, 1992) and it is possible that the RF mapping procedures employed by De Weerd and colleagues resulted in RF contraction before expanded RF borders could be precisely delineated. Thus, climbing activity may be interpreted as either RF expansion or RF gain.

Discrepancies over whether disinhibition induces RF expansion or RF gain may be due, in part, to how the boundaries of a receptive field are defined (Chapman & Stone, 1996; DeAngelis et al., 1995; Fitzpatrick, 2000). However, there is evidence in favor of both proposals even when such methodological issues are accounted for (Chapman & Stone, 1996).

Dissertation Rationale: Neural Mechanisms of Short-Term Visual Plasticity in Humans

The neural mechanisms of short-term visual plasticity were investigated in human subjects using an artificial scotoma paradigm. The study of short-term plasticity in humans presents a considerable obstacle – receptive fields cannot be directly measured. However, it is possible to use changes in perceptual performance and non-invasive measures of cortical activity to assess the neural mechanisms associated with short-term visual plasticity.

In four experiments, psychophysical and electrophysiological measures were used to draw inferences regarding the neural mechanisms underlying short-term plasticity. The specific aim of these examinations was to provide evidence of disinhibition as the neural mechanism of short-term plasticity in humans and to delineate the functional consequences of disinhibition. The following sections describe the logic of using psychophysical and non-invasive neural measures in the investigation of plasticity in humans.

Experiment 1: Short-Term Plasticity & Disinhibition within the TDZ

Experiment 1 examined psychophysical contrast response functions obtained from within the boundaries of an artificial scotoma with the specific goal of determining how receptive field properties within the TDZ changed with the induction of short-term visual plasticity. The process of disinhibition makes specific predictions regarding perceptual-level changes in psychometric contrast response function as do other models of short-term plasticity. Changes in contrast response functions were interpreted with respect to the predictions of disinhibition and competing models of plasticity.

There have been two major proposals regarding the changes in RF properties associated with an artificial scotoma. One proposal suggests that short-term plasticity induces receptive field expansions within the TDZ (RF expansion; Das & Gilbert, 1995; Kapadia et al., 1994; Pettet & Gilbert, 1992). The second (RF gain) suggests that TDZ neurons exhibit response gain and become increasingly sensitive to stimuli within their RF but show no significant change in RF size, shape, or selectivity (DeAngelis et al., 1995).

It is my contention that the consequences of disinhibition within a deafferented TDZ are best described in terms of two separable but dependent processes: one of receptive field expansion and one of neural response gain. As TDZ cells are released from inhibition (i.e., disinhibition through an artificial scotoma), long-range horizontal projections are unmasked. Horizontal connections provide inputs from up to 8 mm away (Gilbert et al., 1996) and their unmasking increases the responsiveness of TDZ neurons to larger regions of visual space. This aspect of disinhibition does not differ from the proposal of RF expansion. In addition to becoming more responsive to distant regions of space, the occurrence of disinhibition also implies that TDZ neurons will exhibit a

general increase in responsiveness. The removal of local inhibition within TDZ not only unmasks existing horizontal inputs but also results a reduction in neural response selectivity. The selectivity of neural response is a function of local inhibition (e.g., Sillito, 1975). Thus, a reduction in local inhibitory drive would, in turn, induce a reduction in stimulus selectivity. However, though selectivity is lost, neural gain will increase because the cell will respond to a broader range of stimuli. This form of neural gain differs from that put forth by the aforementioned RF gain account in that it is a *nonselective* increase in gain. The distinction between these two forms of gain is discussed below. From hereon, the proposal that disinhibition results in receptive field expansions and changes in neural response gain will be referred to as the *disinhibition model* or *two-process disinhibition model.*

The putative proposals of RF expansion, RF gain, and disinhibition models each carry a set of implicit assumptions. A strict account of RF expansion operates on the assumption that, although the size of TDZ receptive fields increases, their internal structure remains intact. That is, only the size of the receptive field has been altered. The cell maintains its response selectivity. For example, if a neuron selective for 45° orientation experienced RF expansion, it would continue to respond to 45° stimuli but would do so over a greater region of space. A strict RF gain model operates on the assumption that there is a multiplicative increase in neural response gain but that there are no changes to the size, shape, or response properties (DeAngelis et al., 1995). Again the cell is assumed to maintain its response selectivity. In this case, if a neuron selective for a 45° orientation were to experience RF gain, it would respond selectively to 45° stimuli within its classic receptive field but would do so more vigorously. This form of neural

response gain will be termed *selective gain* or *selective response gain*. Selective gain has a multiplicative effect on the amplification of the signal to noise ratio of a coded stimulus and is analogous to the form of response gain used to describe the neural mechanisms of selective attention (see Treue, 2001).

There is a distinction between the selective gain implied by the RF gain model and that implied by the disinhibition model. Unlike selective gain, the type of gain predicted by disinhibition is nonspecific. Rather than a response increase to a specific stimulus there is an increase in responding to *any* stimulus. That is, the neuron loses its selective response characteristics and becomes more responsive to stimuli in general. This form of neural gain will be termed *unrestricted gain* (also *unrestricted response gain or unrestricted RF gain*). In the case of unrestricted gain, if a neuron selective for a 45° orientation would increase its response to 45° stimuli but would also increase response to stimuli of other orientations. Note that although unrestricted gain increases absolute neural response rate it would have a detrimental effect in terms of stimulus representation. As neural response selectivity decreases so does the signal-to-noise ratio of a coded stimulus. Thus, computationally speaking, the effect of unrestricted gain is opposite that of selective gain. The results of DeAngelis and colleagues (1995) were such that gain increased in a multiplicative manner. It was assumed that this gain reflected that of selective gain but the data are rather ambiguous regarding neural response selectivity. Thus, the form of gain described in this study may have, in fact, been that of unrestricted gain. If so, then it can be assumed that unrestricted gain has a multiplicative effect on neural response.

The assumptions of RF expansion, RF gain, and disinhibition are described above in terms of single-cell response characteristics. However, each mechanism can be considered in terms of how the population of TDZ neurons exhibiting plasticity would be affected. Predicted changes in the TDZ population response can, in turn, be used to predict the impact of each hypothesis (RF expansion, RF gain, and two-process disinhibition) on perceptual performance (in this case the contrast response function). At the population level, RF expansion predicts that a greater proportion of TDZ neurons will represent a given region of space within the scotoma. Thus, in terms of psychophysical contrast response functions, RF expansion predicts improved perceptual thresholds (leftward shift) within an artificial scotoma due to the increased representation within the TDZ (Figure 2A). According to RF gain, an artificial scotoma should have a multiplicative effect on the TDZ population's selective response gain, thus increasing the signal-to-noise ratio of the coded stimulus. Thus, RF gain implies a multiplicative enhancement in perceptual performance within an artificial scotoma which would be reflected in the contrast response function as an increase in asymptotic performance (Figure 2B; Carrasco, 2006; Ling & Carrasco, 2006). Two-process disinhibition proposes receptive field expansions accompanied by unrestricted gain. A greater population within TDZ would represent a given region of space within the artificial scotoma (due to receptive field expansion) and though this population would exhibit an overall amplification of response rate there will be a reduction in signal-to-noise ratio due to unrestricted gain. Thus, the TDZ population code is a balance of receptive field expansion and unrestricted gain. In terms of psychophysical performance, the two-process disinhibition model predicts a mixture of performance enhancement and

degradation depending on the level of contrast. As discussed previously, RF expansion predicts a reduction in contrast threshold. However, the effects of unrestricted gain are opposite that of selective gain (i.e., RF gain model) and a reduction in asymptotic performance would be expected. Thus, the effects on the contrast response function should reflect a balance of RF expansion and unrestricted gain. Because unrestricted gain is multiplicative, its effects are minimal at lower contrasts. Thus, the effects of RF expansion will dominate the psychometric function and perceptual performance will be enhanced at low contrasts. However, at high contrasts, unrestricted gain is amplified. In this case, the effects of unrestricted gain would dominate the contrast response function and performance should decrease at high levels of contrast. Thus, two-process disinhibition predicts the overall form of the contrast response function to be that of improved contrast thresholds (leftward shift) along with a reduction in asymptotic performance (Figure 2C).

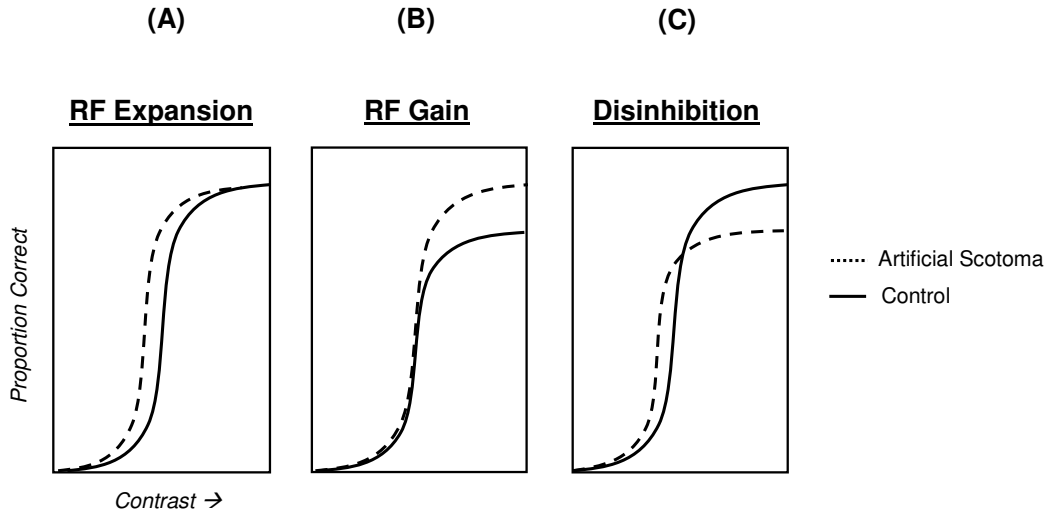

Figure 2. Psychophysical predictions in the contrast response function for (A) RF expansion, (B) RF gain, and (C) disinhibition. The dotted line indicates the contrast response function obtained from within the boundaries of an artificial scotoma relative to some control condition (solid black line).

Experiment 2: Neural Correlates of Short-Term Plasticity within the TDZ

In Experiment 2, cortical responses from within TDZ were measured using event-related potentials. A high contrast visual probe was used to elicit a response from TDZ following a period of conditioning with an artificial scotoma. The resultant visual evoked potential (VEP) was assessed for effects of short-term plasticity.

The goals of Experiment 2 were twofold. One goal was simply to provide a neural correlate of disinhibition within the human visual system. Disinhibition predicts an increase in the neural population representing a region of space as well as an increase in the unrestricted gain of this population. Thus, the mechanism of disinhibition predicts an increase in activity evoked from the TDZ (i.e., amplified visual components). A second goal of Experiment 2 was to provide some indication of where plasticity begins within the human visual system. Some single-cell studies have reported RF expansions in V1 almost immediately after retinal lesions as well as during conditioning with an artificial scotoma (e.g., Gilbert & Wiesel, 1992; Pettet & Gilbert, 1992). However, others have failed to find change in V1 and report changes only in higher visual areas such as V2 and V3 (De Weerd et al., 1995).

In Experiment 2, several sensory components of the visual evoked potential were assessed for plasticity-related changes. Effects within these components were used to provide a crude measure of the earliest level exhibiting plasticity within the human visual hierarchy. Scalp-recorded potentials have poor spatial resolution and their ability to localize activity to specific cortical areas is quite limited. However, an early sensory component of the VEP, the C1, has been repeatedly localized to primary visual cortex (Clark, Fan, & Hillyard, 1995; Di Russo et al., 2001; Jeffreys & Axford, 1972a,b;

Martinez et al., 1999; Martinez, DiRusso, Anllo-Vento, & Hillyard, 2001a; Martinez, DiRusso, Anllo-Vento, Sereno, & Hillyard, 2001b). Human V1 lies within the folds of the calcarine sulcus such that the upper visual field is represented within the lower bank of the sulcus and the lower visual field is represented in the upper bank. The geometric configuration of V1 within the calcarine sulcus imparts a characteristic signature onto the C1 component – it reverses polarity between the upper and lower visual fields (Jeffreys & Axford, 1972a,b; Martinez et al., 1999; Martinez et al., 2001a,b). The C1 can be readily identified by its polarity reversal and can, in turn, be used as an index of plasticity at the level of V1. That is, amplitude amplification of the C1 component that is induced by an artificial scotoma can be assumed to reflect short-term plasticity and disinhibition within a V1-DZ. Later components of the VEP (P1 and N1) arise from extrastriate visual areas. The P1 component arises from activity in extrastriate activity 100 to 150 ms post-stimulus (Di Russo et al., 2001; Martinez et al., 2001a,b). The N1 (150-220 ms) begins directly after P1 and reflects continued extrastriate visual processing (Di Russo et al., 2001). Modulation of P1 and N1 amplitude due to an artificial scotoma can be considered to reflect plasticity in higher-level extrastriate areas.

Experiment 3: Effects of Short-Term Plasticity and Disinhibition within the IZ

Plasticity within TDZ reflects the unmasking of horizontal inputs, a major source of which comes from the region of normal cortex that surrounds the TDZ, the IZ. Because the IZ still receives normal visual input, its activity can be considered to "invade" the TDZ. Experiment 3 was concerned with evaluating how disinhibition within the TDZ affects neural response properties within this surrounding IZ. To investigate this

issue, psychometric contrast response functions were measured from the region of space surrounding an artificial scotoma (i.e., the region of space represented by the IZ). The predictions of disinhibition are less clear for the IZ than the TDZ, as IZ continues to receive normal visual inputs. However, invading activity into the TDZ may be expected to have some measurable perceptual effect on the contrast response function. Like Experiment 1, contrast response functions from Experiment 3 were also evaluated for changes consistent with the predictions of RF expansion, RF gain, and disinhibition.

Experiment 4: Neural Correlates of Invading Activity

Experiment 4 sought a neural correlate of invading activity into TDZ. Following conditioning with an artificial scotoma, VEPs were elicited by stimulating the region of space that surrounded the scotoma (extra-scotoma space). C1, P1, and N1 components were analyzed for effects consistent with invading activity.

CHAPTER 2

EXPERIMENT 1

Experiment 1 used psychophysical measurement to examine the effects of short-term plasticity on receptive field characteristics within the TDZ. Contrast response functions obtained from within the boundaries of an artificial scotoma were used to evaluate three proposals regarding the effects of disinhibition on TDZ receptive field dynamics. Specifically, models of receptive field expansion, neural response gain, and two-process disinhibition were evaluated.

Method

Subjects

Four naïve psychophysical observers (two females) were recruited from the Georgia Institute of Technology undergraduate and graduate population. Subject ages ranged from 19 to 25 (M=21.0, SD=2.7). Each subject's vision was assessed using the automated Freiburg visual acuity test (Bach, 1996). All subjects had normal or corrected to normal vision. Experimentation was conducted under the approval of the Institutional Review Board and with the informed consent of the participant. Subjects were paid $10/hour for their participation. One subject (S04) was excluded from analysis due to excessive ocular activity.

Stimuli and Procedure

Experimentation was conducted in a sound-attenuating chamber under low levels of ambient illumination. Stimuli were presented on a 21-inch CRT monitor using the Presentation stimulus package (Neurobehavioral Systems, Albany, CA). Monitor refresh rate and resolution were 60 Hz and 1024 × 768, respectively. Monitor gamma was corrected in software to a value of 1.0 (linear). Gamma correction was verified through physical measurement of luminance with a photometer. An approximate viewing distance of 57 cm was maintained using a chin rest, so that 1 cm on the screen subtended approximately 1° of visual angle.

Experimental trials consisted of a 6.0 second exposure to a dynamic background stimulus (*conditioning phase*) followed by the presentation of a visual probe that varied in contrast. During the conditioning phase two uniform mid-gray discs (*scotoma discs)* were superimposed upon the dynamic background stimulus, one in the left visual field and one in the right. The introduction and duration of scotoma discs varied with experimental condition. 500 ms prior to the end of the conditioning period a warning stimulus appeared. The warning stimulus consisted of a brief (50 ms) color and luminance change in the fixation dot (from red to white). The conditioning phase terminated with the removal of the dynamic background, leaving only the scotoma discs and a fixation point. This display persisted for a random interval between 300 and 700 ms after which time the visual probe was flashed for 50 ms within the boundaries of one of the two scotoma discs. The visual probe was an intra-scotoma Gabor annulus (described below) that had a slight leftward or rightward tilt. Following another random interval of 300 to 700 ms a question mark ('?') in white text prompted observers for a

response. Subjects were tasked with making a two alternative forced-choice (2 AFC) discrimination regarding the tilt of the Gabor annulus.

Dynamic background stimuli consisted of 1200 small (0.1° × 1.0°), high luminance (137.0 cd/m^2), vertically-oriented bars. These bars were present in random positions on a dark background (33.6 cd/m^2) with a red fixation dot (0.2° × 0.2°) in the center of the display. Each vertical bar was randomly repositioned within a 36° x 26° area every 50 ms (20 Hz) with the restriction that a bar could not be positioned such that it overlapped in space with the fixation dot. Artificial scotoma stimuli were uniform gray discs (75.1 cd/m^2; 2.0° diameter) superimposed upon the dynamic background. Scotoma discs were centered 5.0° from fixation and always occurred in pairs such that a single disc was present in both the left and right visual field. During experimentation the position of scotoma discs alternated between the upper and lower halves of the visual field. Scotoma discs always maintained an eccentricity of 5.0° but were positioned with a polar angle of 25° relative to the horizontal meridian when presented in the upper visual field and at an angle of 45° when presented in the lower visual field. Visual probes were Gabor annuli that consisted of a 5 cpd sinusoidal annulus centered with a Gaussian envelope. For Experiment 1, Gabor annuli were intra-scotoma in that they appeared within the inner boundaries of the scotoma discs (Figure 3). An annulus was chosen as a probe stimulus because the short-term plastic effects of an artificial scotoma are found closest to the borders of the scotoma stimulus (DeWeerd et al., 1995). The sinusoidal phase of Gabor annuli varied randomly between 0º, 30º, 60º, 90º, 120º, and 150º on a trial-by-trial basis to thwart the use of phase information as a cue for discrimination. Gabor annuli had a leftward or rightward tilt between 2 and 4 degrees. Tilt was

determined individually for each subject in a pre-screening session. Intra-scotoma Gabor annuli varied in contrast from 0.09 to 0.64 at 14 logarithmic increments (0.093, 0.098, 0.104, 0.112, 0.122, 0.136, 0.155, 0.180, 0.213, 0.257, 0.316, 0.395, 0.500, and 0.640). Trials contained an equal weighting of each of the 14 contrast levels.

Figure 3. Example intra-scotoma Gabor annulus. In this case the stimulus is high contrast and has a tilt of 45 degrees. In Experiment 1, contrast level was varied and stimulus tilt was set at a value between 2 and 4 degrees from the vertical.

There were two manipulations of theoretical interest. In one condition (the Scotoma condition) an artificial scotoma was induced by superimposing the scotoma discs on the dynamic background for the duration of the conditioning phase (i.e., 6.0 seconds). In a second condition (the Sham condition) the scotoma discs were only introduced for the last 1.0 second of the conditioning phase. That is, the dynamic background stimuli modulated for a period of 5.0 seconds after which time the scotoma discs were superimposed upon the dynamic background for the remaining 1.0 second of the conditioning phase. The perceptual filling-in of an artificial scotoma requires a period of several seconds to occur as do the observed receptive field changes that accompany the illusion (DeWeerd et al., 1998, 2000). Thus, neurophysiological consequences of an artificial scotoma should be largest and most pronounced in the Scotoma condition where the scotoma is conditioned for an extensive period of time. The Sham condition serves as a tightly matched control since the stimulus parameters are

nearly identical with the exception of the duration of scotoma conditioning. The typical sequence of events for Scotoma and Sham trials is depicted graphically in Figure 4.

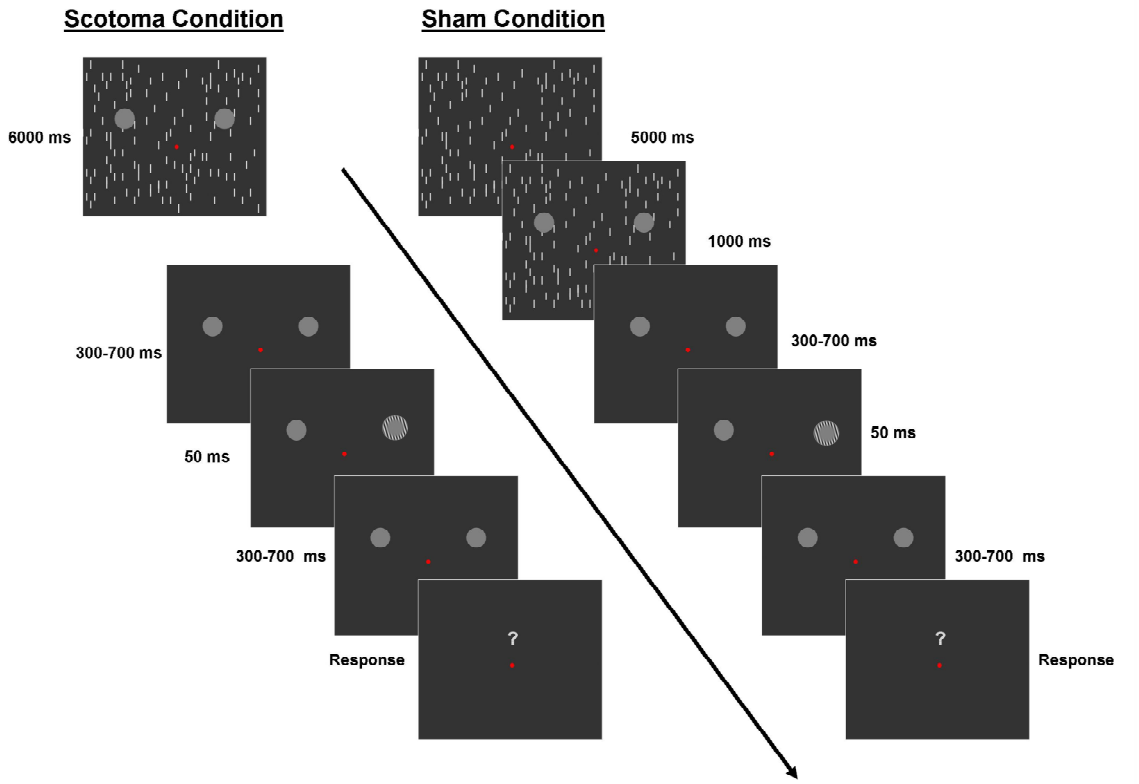

Figure 4. Schematic depiction of the sequence of events for Scotoma and Sham conditions of Experiment 1. In the Scotoma condition, perceptual filling-in of artificial scotomas is induced through a six second conditioning period. The Sham condition served as a control and introduced scotoma discs only in the final one second of the conditioning period.

A third manipulation (Baseline condition) was also included in the experimental design. The baseline measure served simply to obtain a baseline contrast response function used to ensure that sigmoidal and monotonic contrast response functions could be obtained from the Gabor annuli stimuli. The baseline measure consisted of a brief exposure to the dynamic background stimuli (1000 ms) followed by a 500 ms period of a display consisting of the fixation and scotoma discs on the uniform background. The

warning stimulus was then presented for 50 ms and a random period between 800 and 1200 ms passed. A Gabor annulus was then flashed for 50 ms. An additional random period of 300 to 700 ms then transpired after which a question mark prompted the subject for a response. The subjects' task was identical to that of the Scotoma and Sham conditions.

Prior to experimental testing each observer completed a pre-screening session. During this session a brief vision test was administered and a 45-minute test was run to set the tilt of Gabor annuli for each participant such that asymptotic performance was approximately 90% correct. This session also served as an extensive practice to familiarize participants with stimuli and task. The pre-screening test presented 512 trials of the Baseline condition trial type. In this test, Gabor contrast was maintained at the highest experimental level (0.64) whereas annulus tilt was manipulated between 2°, 3°, 4°, or 5°. Average performance for each tilt was calculated and a performance level of 90% was estimated through linear interpolation. The minimum and maximum tilt allowed was 2° and 4°, respectively.

Each observer participated in twelve independent sessions completed on separate days. Each session was approximately two hours in duration. Within a session, trials were blocked by condition (Scotoma, Sham, or Baseline) and further sub-blocked by the position of scotoma discs (upper vs. lower visual field). Before a block was initiated, a 1-minute preconditioning period was given. In the Scotoma condition, this period consisted of the fixation point and scotoma discs presented against the dynamic texture background. The pre-conditioning period for Scotoma and Baseline blocks consisted of only the dynamic texture background. The order of condition blocks was

counterbalanced between sessions according to a Latin square. The order of scotoma disc position (upper vs. lower visual field) was counterbalanced by alternating order between sessions. A total of 8,064 trials were completed in the twelve experimental sessions, yielding 192 trials for each contrast level of the psychometric function.

Upon completion of the sixth session, an approximate evaluation of asymptotic performance was evaluated to ensure that accuracy had not reached ceiling. Accuracy data for the highest level of contrast (0.64) was collapsed across Scotoma, Sham, and Baseline conditions. Subjects whose performance exceeded 95% were rerun in the prescreening session to reset the Gabor tilt to a level of 90%.

Electrooculography

Electrooculogram (EOG) was recorded during each of the experimental psychophysical sessions. The induction of an artificial scotoma necessitates steady fixation and infrequent blinking. Thus, EOG was used to monitor eye movements and blinks during experimentation.

EOG was recorded with a Neuroscan NuAmps amplifier (El Paso, TX). Electrodes were positioned above (X3) and below (X4) the left eye and on the left and right canthus of each eye (X1 and X2, respectively). These four leads were recorded in reference to an electrode placed over the right mastoid process. An electrode positioned in the center of the forehead served as ground. Recordings were digitized at a rate of 500 Hz and low-pass filtered during acquisition at X Hz. Offline, bipolar EOG channels were formed by subtracting X4 from X3 (vertical EOG; VEOG) and X2 from X1 (horizontal EOG; HEOG). VEOG and HEOG were digitally band-pass filtered (0.5 – 50 Hz; 12

dB/oct). Root mean square (RMS) activity was computed over the conditioning phase for both Scotoma and Sham conditions and served as indices of eye movements and blinks for each of the twelve sessions. Specifically, RMS of HEOG was used to assess the degree of eye movement whereas VEOG was used to assess blinks. Additionally, an automated algorithm in the Brain Vision Analyzer EEG analysis software (Brain Products GmbH, Munich, Germany) was used to count the number of blinks during the conditioning phase of each condition. EOG data from one session (#12) of one participant (S02) was corrupt and could not be included in analysis.

Based on RMS and blink counts psychophysical data from one subject (S04) were excluded from analysis. Relative to the other three observers, S04 had excessive VEOG activity, the likely source of which was a high rate of blinking. Blinks and eye movements can impede the perceptual and neurophysiological changes that accompany an artificial scotoma so S04 was dropped from analysis.

Psychophysical Data Analysis

Contrast response functions were analyzed independently for each psychophysical observer. All psychophysical analyses were conducted using custom software written in Matlab (Mathworks, Natick, Massachusetts). Accuracy data were pooled across the twelve experimental sessions for each of the fourteen levels of contrast. Psychometric contrast response functions were obtained for each participant by fitting the Naka-Rushton function to the data (Albrecht & Hamilton, 1982; DeAngelis, Ohzawa, & Freeman, 1993; Ling & Carrasco, 2006; Sclar, Maunsell, & Lennie, 1990).

$$R = \frac{R_{max} \cdot C^n}{C^n + C50^n} + M \quad (1)$$

The Naka-Rushton equation is a quantitative model that captures the neural response rate of neurons within striate cortex to contrast and has been widely used to model psychophysical contrast response functions in humans (e.g., Ling & Carrasco, 2006). In the equation, R is performance, R_{max} is the contrast level at which the response saturates (i.e., the asymptote), C is the contrast level, M is the response at the lowest level of contrast, $C50$ is the contrast at the half-saturation point (i.e., the threshold), and n is the exponent that determines the slope of the response function.

The Naka-Rushton model was fit to accuracy data via maximum likelihood estimation. Threshold ($C50$), asymptote (R_{max}), and slope (n) parameters were allowed to vary freely in these fits. The minimum response parameter (M) was fixed at 0.5 (the chance level of performance in a 2 AFC design). For each observer and condition, threshold, asymptote, and slope parameters were estimated by performing fits to accuracy data averaged over the twelve experimental sessions. Error around each parameter was estimated using a bootstrap method (Efron & Tibshirani, 1993; Wichman & Hill, 2001a,b). Bootstrapping was performed by regenerating many "synthetic" psychophysical data sets through resampling (with replacement) each point of the psychometric function and then fitting each synthetic data set with the Naka-Rushton Equation by maximum likelihood estimation. Such parameter estimates were calculated for 10,000 of such bootstrapped data sets. Bootstrapped parameter estimates were then used to calculate 95% confidence intervals for each parameter of interest. Confidence interval estimation was bias corrected and accelerated (BC_a correction) according to the

procedure described in Efron & Tibsheirani (1993). Statistical inferences regarding parameter differences between Sham and Scotoma conditions were drawn by examining confidence intervals for overlap with mean parameter estimates.

A further analysis of interest compared psychophysical models of RF gain, RF expansion, and disinhibition. Comparison of these three models was accomplished by the incorporation of two additional parameters (rf_e and rf_g) into the Naka-Rushton equation. RF expansion was modeled with equation (2).

$$R = \frac{R_{max} \cdot (rf_e \cdot C^n)}{(rf_e \cdot C^n) + C50^n} + M \qquad (2)$$

With the exception of rf_e, all parameters are identical to the original Naka-Rushton equation (Equation 1). The parameter rf_e represents receptive field expansion and affects the horizontal position constrast response function. The expansion of receptive fields within TDZ results in a larger proportion of neurons that respond to a particular region of space and a reduction in contrast threshold would be expected.

Changes in response gain were expressed as the equation:

$$R = rf_g \cdot \frac{R_{max} \cdot C^n}{C^n + C50^n} + M \qquad (3)$$

.

Here, the rf_g parameter represents a multiplicative gain effect. The major effect of a multiplicative change in gain is a shift in asymptote of the contrast response function. A value of rf_g greater than one (asymptote increase) is indicative of *selective response gain* where cells exhibit increases in gain but maintain their response selectivity. That is, there is an improvement in perceptual performance at higher contrast levels. A value of rf_g less

than one (asymptote decrease) is indicative of *unrestricted response gain* where cells exhibit nonspecific increases in gain.

Lastly, Equation 4 is a hybrid model of receptive field expansions and changes in response gain. This equation contains both rf_e and rf_g parameters. Such a model can capture the combined effects of receptive field expansion and response gain.

$$R = rf_g \cdot \frac{R_{max} \cdot (rf_e \cdot C^n)}{(rf_e \cdot C^n) + C50^n} + M \quad (4)$$

Quantitative models were fit to each observer's data by maximum likelihood estimation. Initial parameter estimates obtained from the fit to the Sham condition were used to set R_{max}, $C50$, and n. M was fixed at 0.5. Fits of the two-parameter rf_e/rf_g model were evaluated against the reduced one-parameter rf_e and rf_g models using a nested hypothesis F-test (Equation 5; Lu & Dosher, 1998).

$$F(df_1, df_2) = \frac{(R^2_{full} - R^2_{reduced}) / df_1}{(1 - R^2_{full}) / df_2} \quad (5)$$

Here, df_1 is the number of free parameters in the full model less the number of parameters in the reduced model and df_2 is the number of data points fit by each model minus the number of free parameters in the full model less one. Thus, for fits conducted in Experiment 1, $df_1 = 1$ and $df_2 = 11$. The test described by equation 5 was performed once to evaluate the fit of the two-parameter rf_e/rf_g model against the rf_e model and again to evaluate the fit of the two-parameter rf_e/rf_g model against the rf_g model. The rf_e/rf_g model was considered to be superior if both F-tests revealed it to be statistically superior to the one-parameter models.

Results

Bootstrap Parameter Estimates

Bootstrapping results were consistent with the previously described predictions of disinhibition as two out of three observers exhibited significant threshold and slope reductions. Fits of the Naka-Rushton equation to experimental data are shown in Figure 5A for each of the three observers (S01, S02, and S03). Parameter estimation and 95% confidence intervals for *C50* (threshold), R_{max} (asymptote), and *n* (slope) are depicted graphically in Figure 5B. All comparisons evaluated changes in Scotoma parameters relative to Sham. Evaluation of bootstrapped confidence intervals revealed significant differences in threshold, asymptote, and slope in a subset of observers (Figure 5B). S01 had a significant reduction in asymptote in the Scotoma condition. S02 displayed a significant reduction in both threshold and asymptote but had no measurable change in slope. S03 exhibited significant reductions in threshold and slope in the Scotoma condition but had no statistically significant difference in asymptotic performance.

Quantitative Model Evaluation

An additional analysis of interest was the evaluation of three quantitative models to determine which proposal of short-term plasticity best accounted for psychophysical data. Fits of each quantitative model for each observer are shown in Figure 6. The general pattern of results suggests that changes in the Scotoma contrast response function were consistent with the two-process disinhibition model. For two of the three psychophysical observers (S02 and S03), the disinhibition model yielded superior fits to the data. Nested hypothesis tests revealed significantly better fits for the two-parameter

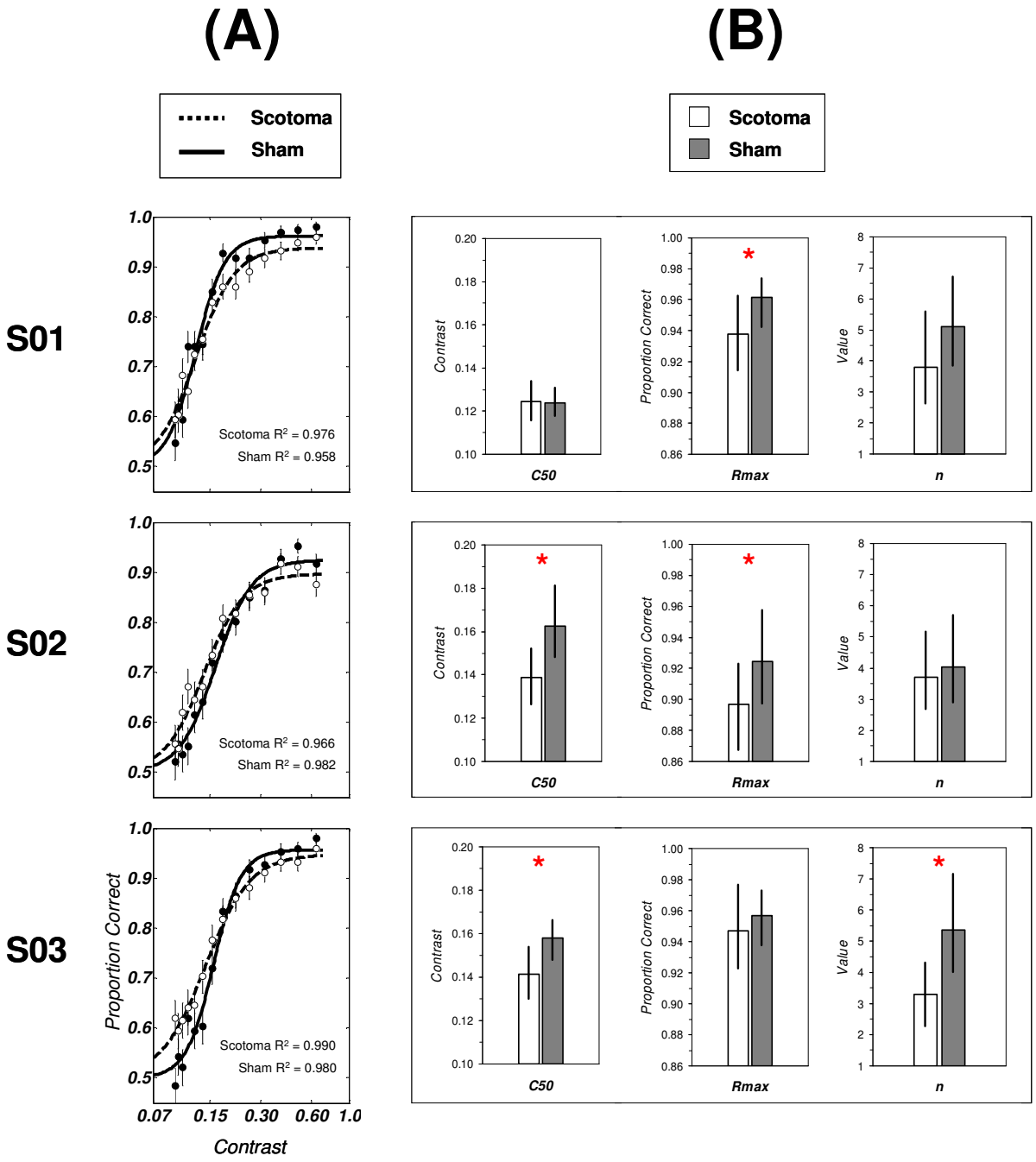

Figure 5. Contrast response functions and parameter bootstrapping from Experiment 1. (A) shows fits to the Naka-Rushton equation for each of the three psychophysical observers. R^2 values are given for fits to the two conditions (Scotoma and Sham). Error bars denote ±1 SD of the 10,000 bootstrap datasets. Contrast level is plotted on a logarithmic scale. (B) plots the estimation and bootstrap estimation of 95% confidence intervals for parameters of interest *C50* (threshold)), R_{max} (asymptote), and *n* (slope). Asterisks denote statistically significant differences between Scotoma and Sham conditions for a given parameter.

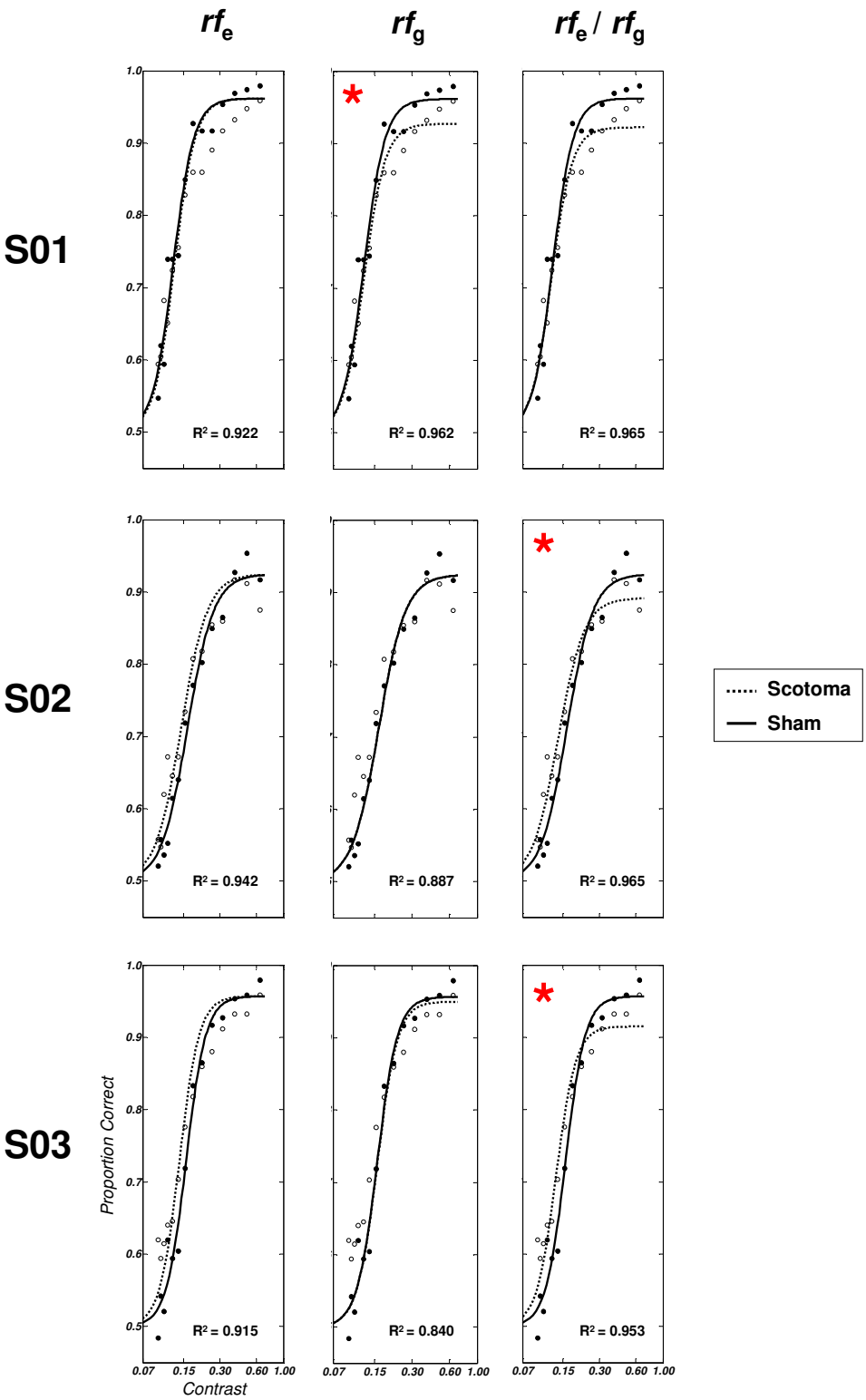

Figure 6. Fits of the three quantitative models to observers in Experiment 1. Contrast level is plotted on a logarithmic scale. R^2 values for the fit of each model are given within their respective panels. The superior model for each observer is indicated by an asterisk (as determined by nested-hypothesis test). Two out of the three observers were best accounted for by the hybrid rfe/rfg model.

rf_e/rf_g model over the rf_e model, S02: F(1,11) = 7.05, p<.05, S03: F(1,11)=8.75, p<.05, and the rf_g model, S02: F(1,11)=24.16, p<.0005, S03: F(1,11)=26.36, p<.0005. For observer S01, the disinhibition model showed an advantage over the rf_e model, F(1,11)=13.45, p<.005, but did not differ from the rf_g model, F(1,11)=1.01, p>.30.

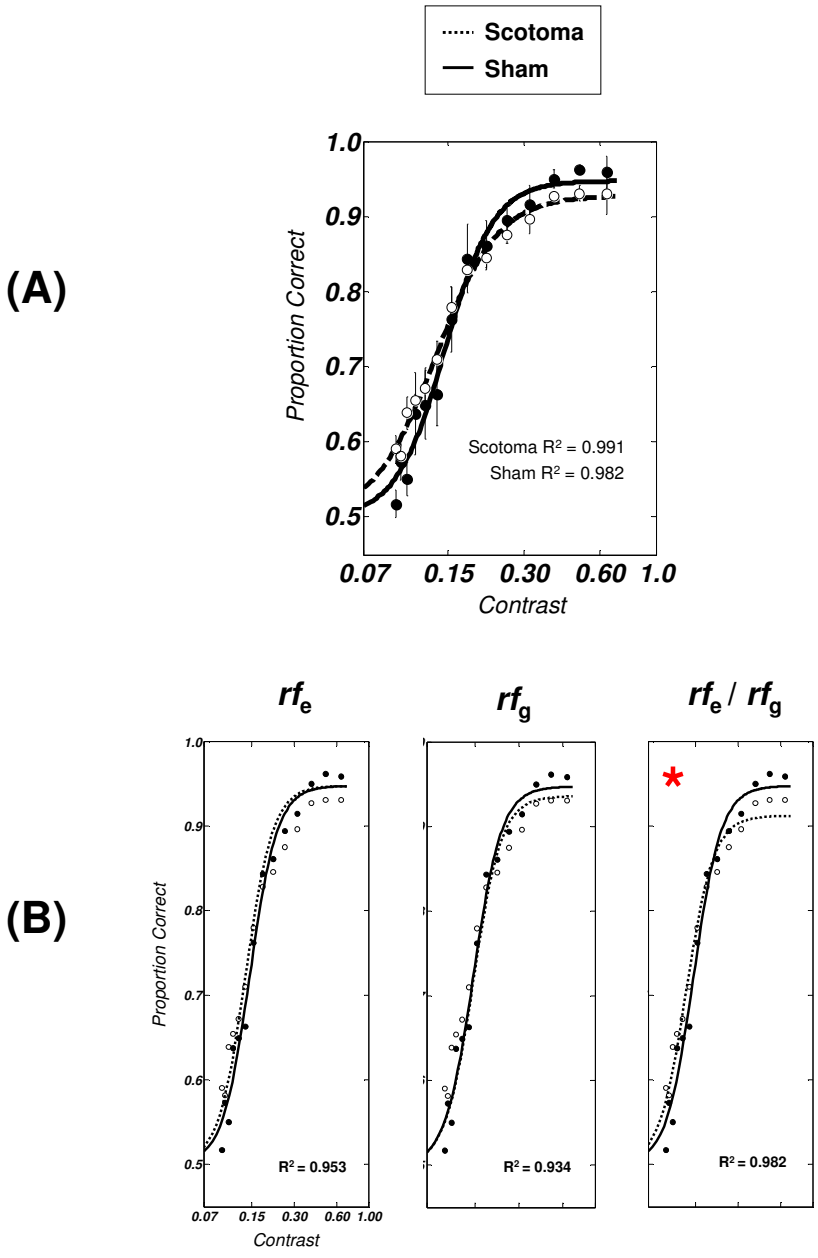

Figure 7. Contrast response function (A) and quantitative model fits (B) for the data averaged across the three observers from Experiment 1. Data were best accounted for by the hybrid rf_e/rf_g model as indicated by asterisk.

S01's data was best described by the model with fewer parameters (i.e., the rf_g model). However, note that the data (and model fit) are indicative of unrestricted gain rather than selective gain. If the artificial scotoma were to induce the selective gain predicted by a strict RF gain model then asymptotic performance should be *increased* for the Scotoma condition relative to Sham. However, S01 displayed the opposite effect, having a reduced asymptote for Scotoma relative to Sham.

Evaluation of the three quantitative models was also performed on the average data of the three psychophysical observers (Figure 7). Nested hypothesis tests revealed the hybrid rf_e/rf_g model to be superior to one-paramter rf_e and rf_g models, $F(1,11)=17.75$, $p<.005$ and $F(1,11)=29.91$, $p<.0005$, respectively.

Effects of practice over the twelve sessions were assessed for each psychophysical observer in Experiment 1. There were no significant or systematic differences between Scotoma and Sham conditions (Appendix A).

Discussion

The short-term plasticity accompanying an artificial scotoma has been proposed to occur as either a result of receptive field expansions (Das & Gilbert, 1995b; Pettet & Gilbert, 1992) or selective neural response gain (DeAngelis et al., 1995). These proposals both attribute change in receptive field dynamics to the unmasking of long-range horizontal connections but do not fully consider the impact of disinhibition on receptive field structure and neural response properties.

Disinhibition predicts that cells within the TDZ will exhibit modulations of both receptive field size and neural response gain. The proposed two-process model of

disinhibition suggests an expansion in RF size due to an increase in the efficacy of long-range horizontal inputs from cortical regions with non-overlapping receptive fields as well as a *nonspecific* increase in neural response gain (unrestricted gain) due to an activity-dependent reduction in local inhibitory drive (Tremere et al., 2003, 2005).

Experiment 1 assessed the predictions of disinhibition on psychophysical performance. Contrast response functions were measured within the boundaries of an artificial scotoma (Scotoma condition) and were compared to those of a control condition (Sham). As discussed previously, disinhibition predicts a leftward shift in the contrast response function (a reduction in threshold) due to the expansion of receptive fields. This threshold reduction would be coupled with a reduction in asymptotic performance due to an increase in unrestricted gain.

Results of Experiment 1 were highly consistent with a disinhibition model of short-term plasticity within the TDZ. Bootstrap estimation of psychometric parameter error showed that two out of three observers (S02 and S03) exhibited a significant reduction in contrast threshold. Two out of three observers (S01 and S02) also exhibited a significant reduction in asymptote.

Quantitative modeling revealed that the disinhibition model best accounted for every observer's data. The two-parameter rf_e/rf_g model provided a superior fit to the average data of the three observers, consistent with two-process disinhibition. Individual subject fits revealed the two-parameter rf_e/rf_g model to provide a superior fit in two observers (S02 and S03). In one observer (S01), the one-parameter rf_g model provided the best fit. However, this fit was such that asymptote was reduced rather than amplified,

consistent with the occurrence of unrestricted gain rather than selective gain. Thus, the data of S01 are best explained by two-process disinhibition rather than RF gain.

The lack of threshold change in S01, and superior fit of a one-parameter RF gain model, may be partly attributable to the range of contrasts tested. S01's performance at the lowest contrasts was considerably better than that of S02 and S03. Because of this increased perceptual sensitivity, the range of contrasts tested may have not have been ideal to detect leftward shifts in threshold as these would be driven mainly by increased perceptual performance at lower contrasts. Similarly, the range of contrasts tested may have been partially responsible for S03's lack of difference in asymptotic performance found by bootstrap estimation. S03's performance at lower contrasts remained above chance in the Scotoma condition and was likely the cause of the decreased slope estimate for the Scotoma condition. This decreased slope, in turn, affects the estimate of asymptote and this may account for the lack of statistical difference in $R_{\max}$ for S03.

The results presented here are consistent with the predictions of the two-process disinhibition model and suggest that that both receptive field expansion and unrestricted gain are induced in the TDZ through disinhibition. Such a two-process disinhibition model provides a resolution to the debate of RF expansion versus RF gain as it can account for the single-cell results reported by studies in support of either proposal (e.g., DeAngelis et al., 1995; Pettet & Gilbert). The two-process disinhibition model also accounts for two important findings in the psychophysical examination of artificial scotomas in humans. One psychophysical investigation reported a perceptual correlate of receptive field expansions following an artificial scotoma by demonstrating a perceptual compression of space within the boundaries of an artificial scotoma (Kapadia et al.,

1994). As the two-process model too proposes the occurrence of RF expansions, it would also predict such a result. A more recent psychophysical examination has reported a quite different interpretation of the effects of an artificial scotoma on visual perception. Mihaylov, Manahilov, Simpson, and Strang (2007) used a perceptual template model to explain visual aftereffects that accompany an artificial scotoma conditioned at the fovea. Their results suggested that the effect of an artificial scotoma was such that it increased internal noise within the perceptual system (see Dosher & Lu, 1999). Though receptive field expansions cannot account for such a result, this increased "internal noise" is highly consistent with the process of unrestricted gain proposed by the two-process disinhibition model. That is, unrestricted gain has an effect of reducing the signal-to-noise ratio of a coded stimulus due to a loss of neural response selectivity.

CHAPTER 3

EXPERIMENT 2

Experiment 2 investigated the neural correlates of short-term plasticity and disinhibition. Event-related potentials were elicited from within the boundaries of a conditioned artificial scotoma using a high-contrast visual probe. VEPs obtained from within an artificial scotoma were examined relative to a control condition for amplitude fluctuations consistent with disinhibition. The C1, P1, and N1 components were examined.

Method

Subjects

Eighteen naïve subjects (10 females) ranging in age from 18 to 22 (M=19.5, SD=1.0) were recruited from the Georgia Institute of Technology undergraduate population. All subjects reported normal or corrected to normal vision and gave informed consent prior to participation. Each subject participated in two independent sessions conducted on separate days. Three of the eighteen subjects were subsequently dropped due to poor signal-to-noise ratio of ERPs.

Stimuli and Procedure

Stimuli were identical to that of Experiment 1 with the exception that the contrast level of Gabor annuli were maintained at a constant contrast of 0.8 to improve the quality of ERP recordings. A total of 1,344 trials were collected across the two experiment

sessions. Trials were blocked by condition (Scotoma, Sham, or Baseline) and further sub-blocked by the visual field of scotoma conditioning (upper vs. lower). The order of condition blocks remained the same between the two sessions but the order of visual field presentation was reversed between the first and second sessions. A Latin square design was used to counterbalance the order of condition blocks between subjects. A one-minute conditioning period (as described in Experiment 1) preceded the first block of each condition and was repeated after the third block of each condition.

Electroencephalography

Scalp-recorded EEG will be sampled at 1024 Hz from 34 Ag-AgCl electrodes using the ActiveTwo amplifier system (BioSemi, Amsterdam, Netherlands). Electrodes were placed in the following positions according to a modified 10-20 system. Standard 10-20 positions were: FP1, FP2, F7, F8, F3, F4, Fz,, C3, C4, Cz, P7, P8, P3, P4, Pz, T7, T8, O1, Oz, O2, M1, and M2. Additional 10-10 positions were: AF3, AF4, FC1, FC2, FC5, FC6, CP1, CP2, CP5, CP6, PO3, and PO4. Four additional electrodes were placed above and below the left eye and on the outer canthi of the left and right eyes. These leads were used to form bipolar channels for vertical electrooculogram (VEOG) and horizontal electrooculogram (HEOG), respectively.

The ActiveTwo system replaces traditional reference and ground electrodes with common mode sense (CMS) and driven right leg (DRL) electrodes. Because of this arrangement, electrophysiological signals are always acquired in reference to the CMS electrode and all referencing is done offline. The ActiveTwo performs no analog filtering

during data acquisition. The bandwidth of the acquired data has only an upper limit determined by the sampling frequency (268 Hz at a sampling rate of 1024 Hz).

Offline, data were re-referenced to the average of the two mastoid channels (M1 and M2) and digitally band-pass filtered from 1.0 to 40 Hz (12 dB/oct). Stimulus onsets were corrected for timing due to the delay of monitor raster scan. EEG data were epoched into segments of 800 ms, beginning 200 ms before stimulus onset and persisting for 600 ms thereafter. Individual segments were baseline corrected by setting the average of the 200 ms prestimulus interval to zero. Segments were considered artifacts and rejected from analysis if activity in any scalp or EOG channel exceeded ±100 μV. Segmented data were averaged by quadrant of stimulus presentation and condition (Sham, Scotoma, and Baseline). Separate averages were formed for the two sessions. Averages from the two sessions were then averaged together. Average waveforms across the two sessions were low-pass filtered at 40 Hz (24 dB/oct) and baseline corrected by setting the average voltage of the prestimulus interval to zero.

Data Analysis

Three components of the VEP were analyzed for changes in amplitude: C1, P1, and N1. For analysis of each component, data were collapsed across the four quadrants of stimulus presentation. Each component of interest was quantified as the average amplitude within a particular time window. Time windows were determined by inspection of grand average waveforms and topographic scalp maps collapsed across the two experimental conditions (Scotoma and Sham).

The C1 component peaked between 105 and 140 ms. This time window was determined initially by inspection of grand average waveforms for the characteristic polarity reversal between upper and lower visual fields (negative-going for upper visual field and positive-going for lower visual field; Jeffreys & Axford, 1972a; Di Russo et al., 2001). The 105 – 140 ms time window was confirmed through assessment of scalp topographies. The C1 component was clearly present, exhibiting a reversal in voltage between upper and lower visual fields. However, a persisting negativity was apparent within the C1 time window rendering the absolute values the component negative despite the fact that their relative difference was that of a polarity reversal. The cause of this early negativity is unclear but it had no bearing on measurement and quantification of the C1. However, because absolute values of upper and lower C1 were negative, proper visualization of C1 voltage topographies was impossible given the data in its raw form. A simple baseline correction was performed on the averaged data to allow assessment of scalp topographies and verification of the C1 time window, setting a 20 ms interval (65 – 85 ms) preceding the C1 to an average of zero. This had the effect of re-centering the zero-point of the waveform, shifting the entire waveform in the positive direction thus allowing C1 scalp topographies to be visualized and verified. Note that this simple correction to the data was only performed to visualize C1 topographies. All C1 quantification and analysis was performed on the raw waveforms.

Prior to analysis, C1 data were collapsed across left and right visual fields. This was accomplished by re-labeling electrodes according to their contralateral or ipsilateral position relative to the visual stimulus and then averaging these re-labeled electrodes

across left and right visual fields. Due to variations in polarity and scalp topography, data were collapsed separately for upper and lower visual field stimuli.

Analysis of C1 data consisted of an average double subtraction score of Sham and Scotoma conditions tested against zero. Because C1 polarity is inverted between upper and lower visual fields changes in amplitude would be expected to occur in opposite directions. That is, if C1 amplitude were to increase amplitude would become more negative for upper field stimuli and more positive for lower field stimuli. Thus, there would be a net effect of zero between upper and lower visual fields. In order to preserve the relative change in C1 data were aggregated between upper and lower fields by taking the average of a double subtraction. Condition difference scores were calculated separately for upper and lower visual fields by subtracting Sham amplitude from Scotoma amplitude. A second subtraction was then performed between lower and upper visual fields (lower – upper). Because scalp topography shifts between upper and lower field stimuli this subtraction was performed on contralateral electrodes for lower field stimuli and on ipsilateral electrodes for upper field stimuli. The result of the second subtraction was then divided by two to obtain the average condition difference of lower and upper fields. Equation 6 summarizes the procedure for collapsing C1 data across upper and lower visual fields.

$$C1_{\text{diff}} = \frac{(C1_{\text{scotoma}} - C1_{\text{sham}})_{\text{lower}} - (C1_{\text{scotoma}} - C1_{\text{sham}})_{\text{upper}}}{2} \qquad (6)$$

The value of $C1_{\text{diff}}$ summarizes the net effect of C1 amplitude amplification between upper and lower visual fields. A positive value of $C1_{\text{diff}}$ indicates C1 amplification in the Scotoma condition whereas a negative value indicates C1

attenuation. A zero value indicates no difference between the two conditions. Statistical inferences regarding changes in C1 were made through a one-sample t-test of $C1_{\text{diff}}$ against zero. This comparison was made at four electrode locations: CP1/2, P3/4, PO3/4, and Pz. These positions were chosen for analysis based on C1 scalp topography.

P1 and N1 components were determined to peak with the time windows 130-165 ms and 190- 240 ms, respectively. These time windows were determined by inspection of grand average waveforms and scalp distributions collapsed across the four visual quadrants of stimulation. Data were collapsed between upper and lower visual fields by simple averaging. Collapsing across left and right visual fields was accomplished by averaging data according to the position of the electrode (contralateral or ipsilateral) relative to the visual field of stimulus presentation. Paired-samples t-tests were used to draw statistical inferences regarding amplitude differences in the P1 and N1 components. T-tests compared amplitudes of Scotoma and Sham conditions at electrodes O1/2 and P7/8 and were conducted independently for P1 (130-165 ms) and N1 (190-240 ms).

Results

Behavioral Data

The behavioral task of Experiment 2 was such that subjects had to make a discrimination of the tilt of a high-contrast (0.80) intra-scotoma Gabor annulus. A paired-samples t-test was used to compare accuracy between Scotoma and Sham conditions. Mean accuracy in the Scotoma and Sham conditions was 0.905 (SD=0.056) and 0.925 (SD=0.059), respectively. Though statistical significance was not achieved

there was a marginally significant difference between the two conditions, t(14)=-1.91, p<.08.

C1 Component

The C1 component exhibits a shift in scalp topography between upper and lower visual fields, having a negative ipsilateral distribution for upper visual field stimuli and a positive contralateral distribution for lower visual field stimuli (Di Russo et al., 2001). C1 scalp distributions clearly demonstrated such a pattern within the 105 – 140 ms range, confirming this time window as the C1 component (Figure 8).

A significant positive $C1_{diff}$ value was present at electrode P3/4, t(14)=2.24, p<.05, indicating significant amplitude amplification of the C1 for the Scotoma relative to the Sham condition. Marginally significant effects were also present at electrodes CP1/2, t(14)=2.04, p<.07, and Pz, t(14)=1.93, p<.08. No difference was present at electrode PO3/4, t(14)=1.641, p>.12. Values of $C1_{diff}$ are plotted in Figure 9 for each of the tested electrodes.

P1 Component

P1 amplitude was significantly greater in the Scotoma condition than in the Sham condition. This amplitude difference was apparent at contralateral electrode O1/2, t(14)=2.93, p<.05. A marginally significant difference was also present at contralateral P7/8, t(14)=2.09, p<.06. Figure 10 shows P1 scalp topographies and waveforms of illustrating P1 differences.

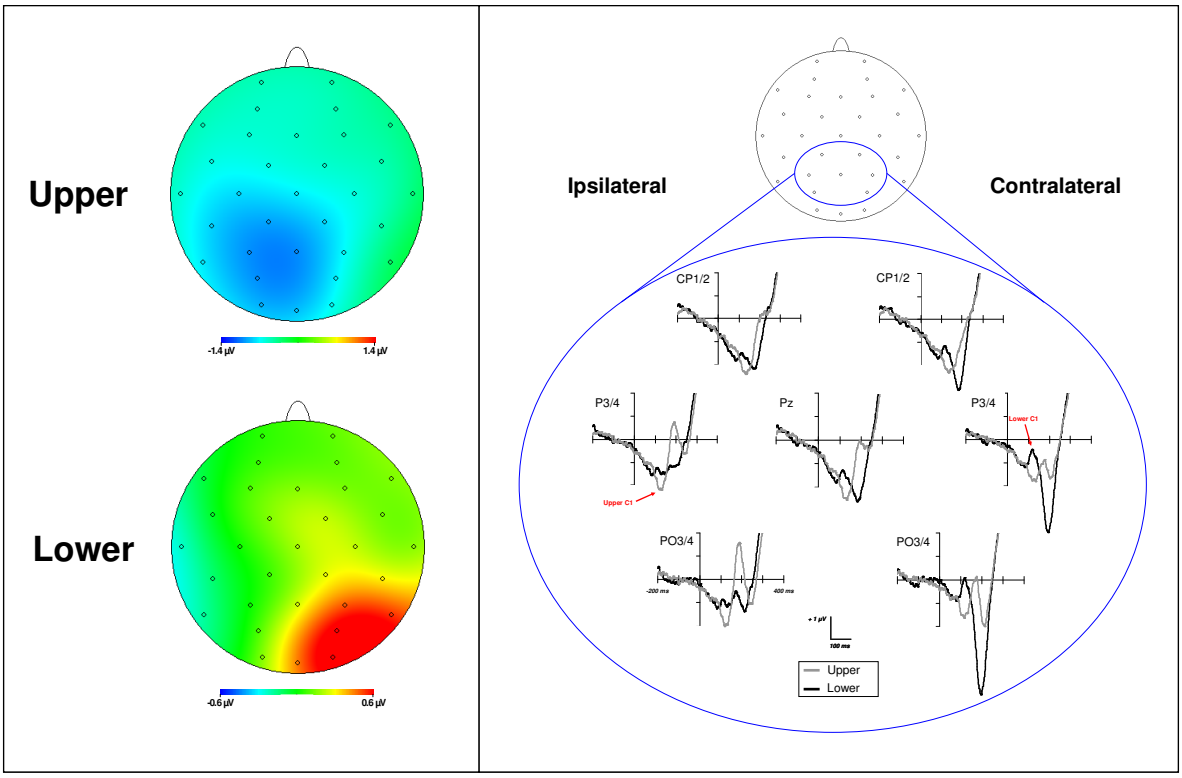

Figure 8. C1 component from Experiment 2. Grand average scalp distributions of the C1 component (105 – 140 ms) are collapsed across left and right visual fields (left panel). Scalp distributions are arbitrarily mapped such that ipsilateral electrode positions are represented on the left and contralateral on the right. Grand average waveforms for upper and lower fields are shown in the right panel. Scalp distributions and waveforms clearly demonstrate a polarity reversal and shift in scalp distribution typical of the C1 component.

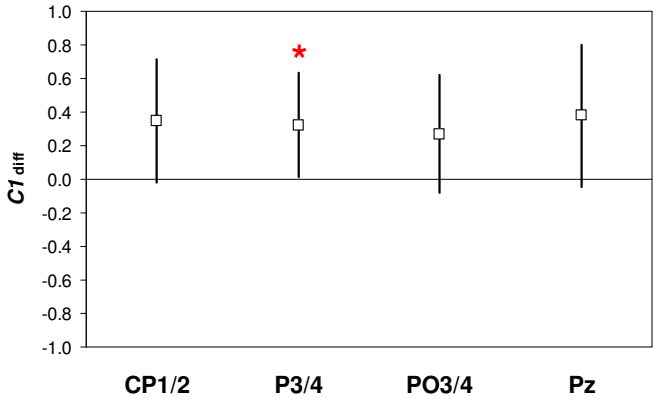

Figure 9. Values of $C1_{diff}$ from Experiment 2. $C1_{diff}$ provides a single measure describing changes in C1 amplitude across the four visual quadrants of stimulation. Positive values of $C1_{diff}$ indicate an increase in C1 amplitude in the Scotoma condition relative to the Sham condition. Negative values indicate a decrease and a value of zero indicates no change. Each of the electrodes tested exhibits a positive $C1_{diff}$ value. Statistical significance was only present at electrode P3/4. Error bars represent 95% confidence intervals.

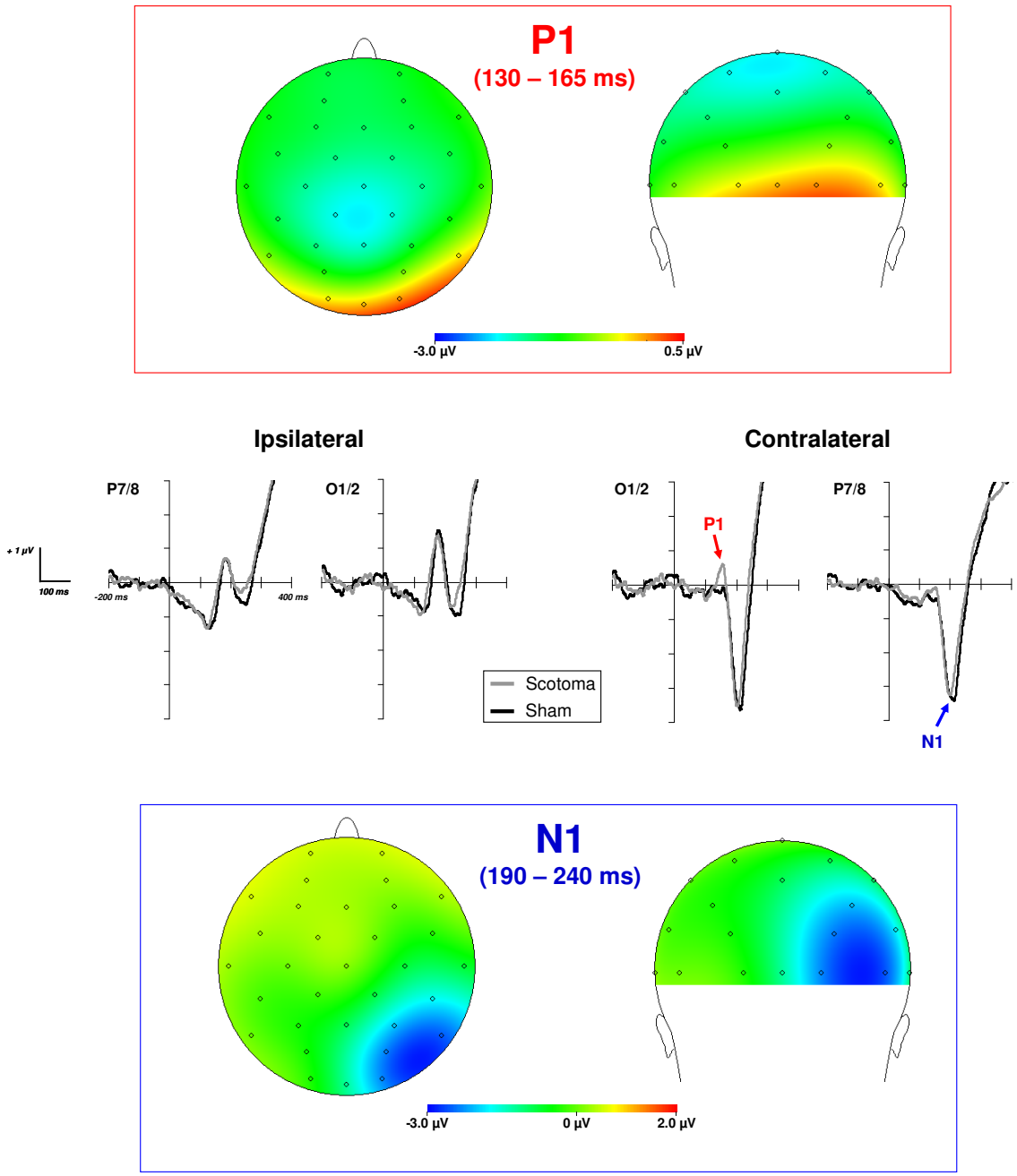

Figure 10. P1 and N1 components from Experiment 2. Grand average scalp topographies of the contralateral P1 and N1 components are shown in the top and bottom panels, respectively. Waveforms are collapsed across visual quadrants (middle). Scalp distributions are arbitrarily mapped such that ipsilateral electrode positions are represented on the left and contralateral on the right. Waveform plots show a clear P1 amplitude enhancement in the Scotoma condition at contralateral O1/2 and an attenuation of N1 amplitude at P7/8.

N1 Component

N1 amplitude was significantly attenuated in the Scotoma condition relative to the Sham condition, contralateral P7/8: $t(14)=2.31$, $p<.05$. There was no statistically significant at contralateral O1/2, $t(14)=1.73$, $p>.10$. Figure 10 plots N1 scalp maps and amplitude differences.

Discussion

Experiment 2 examined the neural correlates of short-term plasticity with the TDZ using event-related potentials. VEPs were recorded in response to visual probes presented within the boundaries of an artificial scotoma (Scotoma condition) and were evaluated relative to a control condition (Sham condition). The goals of Experiment 2 were to 1) provide a neural correlate of disinhibition, and 2) determine the earliest level of the visual hierarchy at which such plasticity may be found.

C1 and P1 amplitudes were significantly amplified in the Scotoma condition. That is, amplitude of C1 and P1 components was increased relative to the Sham condition. These results are consistent with the occurrence of disinhibition within the TDZ. The enhanced amplitude of the C1 and P1 components is consistent with disinhibition within TDZ.

Conditioning of an artificial scotoma also had a significant effect on the amplitude of the N1 component. However, this effect was one of amplitude attenuation rather than amplification. The interpretation of such an effect in terms of disinhibition is difficult given the effects found in C1 and P1. One possibility is that the reduction in N1

amplitude is due to a sustained positivity that overlaps with the N1 time window. Such an effect could arise were disinhibition to induce sustained activity within cortical areas that generate the P1 component. However, such an interpretation cannot be confirmed without further experimentation. The effects of C1 and P1 amplification are the most appropriate indices of short-term plasticity and disinhibition given the current data set.

Single-cell studies of artificial scotomas have led to somewhat discrepant results regarding the earliest cortical visual area at which short-term plasticity may be found. Some studies have found evidence of short-term plasticity within V1 (Pettet & Gilbert, 1992) whereas others have only found effects in higher-level extrastriate areas (e.g., De Weerd et al., 1995). The C1 component has been repeatedly localized to V1 (see Di Russo et al., 2001). Thus, the amplification of C1 suggests that short-term plasticity does occur at the level of primary visual cortex within the human visual system. Amplification of the P1 component further suggests that plasticity and disinhibition are apparent later in the visual hierarchy.

CHAPTER 4

EXPERIMENT 3

Experiment 3 was an exploratory investigation to examine the perceptual consequences of invading activity from invading cortical zone, IZ, into the TDZ. Because the TDZ receives horizontal inputs from the IZ perceptual enhancement or distortion may be expected as a result of this increased representation of extra-scotoma space. Contrast response functions were measured from the region of space surrounding the scotoma (i.e., the region of space represented by the IZ) and were evaluated for changes in perceptual performance associated with invading activity from the IZ.

Method

Subjects

Four naïve psychophysical observers were recruited from the Georgia Institute of Technology undergraduate and graduate population. None of the observers had previously participated in Experiment 1. Subject ages ranged between 19 and 38 (M=26.8, SD=8.2). All observers had normal or corrected to normal vision. One subject (S04) was excluded from analysis due to excessive ocular activity.

Stimuli and Procedure

The stimuli and procedure of Experiment 3 were identical to that of Experiment 1 with two exceptions. First, Gabor annuli probes were extra-scotoma rather than intra-scotoma (Figure 11). That is, Gabor annuli were configured such that the scotoma disc

was contained within annuli's inner radius. Thus, the extra-scotoma Gabor annuli probed the region of space just outside the scotoma boundary. A second variation between Experiment 1 and 3 was the use of a different contrast range to obtain the contrast response function. Extensive pilot testing revealed that the 14 contrast levels used in Experiment 1 did not provide an acceptable range of performance for extra-scotoma Gabor annuli. Specifically, piloting indicated that performance was too high at the lower levels of contrast such that thresholds could not be estimated appropriately. The minimum contrast level was lowered to remedy this issue. Contrast levels were set at 14 logarithmic increments between 0.04 and 0.64 (0.043, 0.048, 0.054, 0.062, 0.073, 0.088, 0.108, 0.135, 0.171, 0.219, 0.283, 0.370, 0.485, and 0.6400).

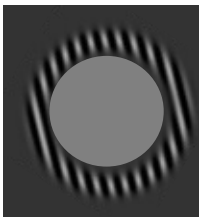

Figure 11. Example of an extra-scotoma Gabor annulus.

Electrooculography

EOG recording and analysis was identical to that of Experiment 1. EOG data from one session of one subject (S04) was corrupt and could not be included in analysis. One psychophysical observer (S04) displayed an excessive degree of activity within the VEOG channel. As with Experiment 1, the source of this VEOG activity was attributable to an excessively high rate of blinking and S04 was excluded from psychophysical analysis.

Psychophysical Data Analysis

Psychophysical data analysis was identical to that of Experiment 1.

Results

Bootstrap Parameter Estimates

Fits of the Naka-Rushton equation to experimental data are shown in Figure 12A for the three psychophysical observers (S01, S02, and S03). Parameter error and estimates are plotted in Figure 12B. Comparison of bootstrapped confidence intervals to mean parameter estimates revealed that none of the observers showed differences in threshold, asymptote, or slope (Figure 12A).

Quantitative Model Evaluation

None of the three quantitative models (rf_e, rf_g, and rf_e/rf_g) accounted for differences between Scotoma and Sham conditions significantly better than the others. A nested-hypothesis test revealed that the hybrid rf_e/rf_g model was not superior to the rf_e model, S01: $F(1,11)=0.594$, $p>.45$, S02: $F(1,11)=3.20$, $p>.10$, S03: $F(1,11)=0.512$, $p>.45$, or the rf_g model, S01: $F(1,11)=2.31$, $p>.15$, S02: $F(1,11)=1.23$, $p>.29$, S03: $F(1,11)=0.512$, $p>.48$. No convincing differences were present between rf_e and rf_g models either. R^2 differences were less that .01 for each subject. Model fits for each observer are shown in Figure 13.

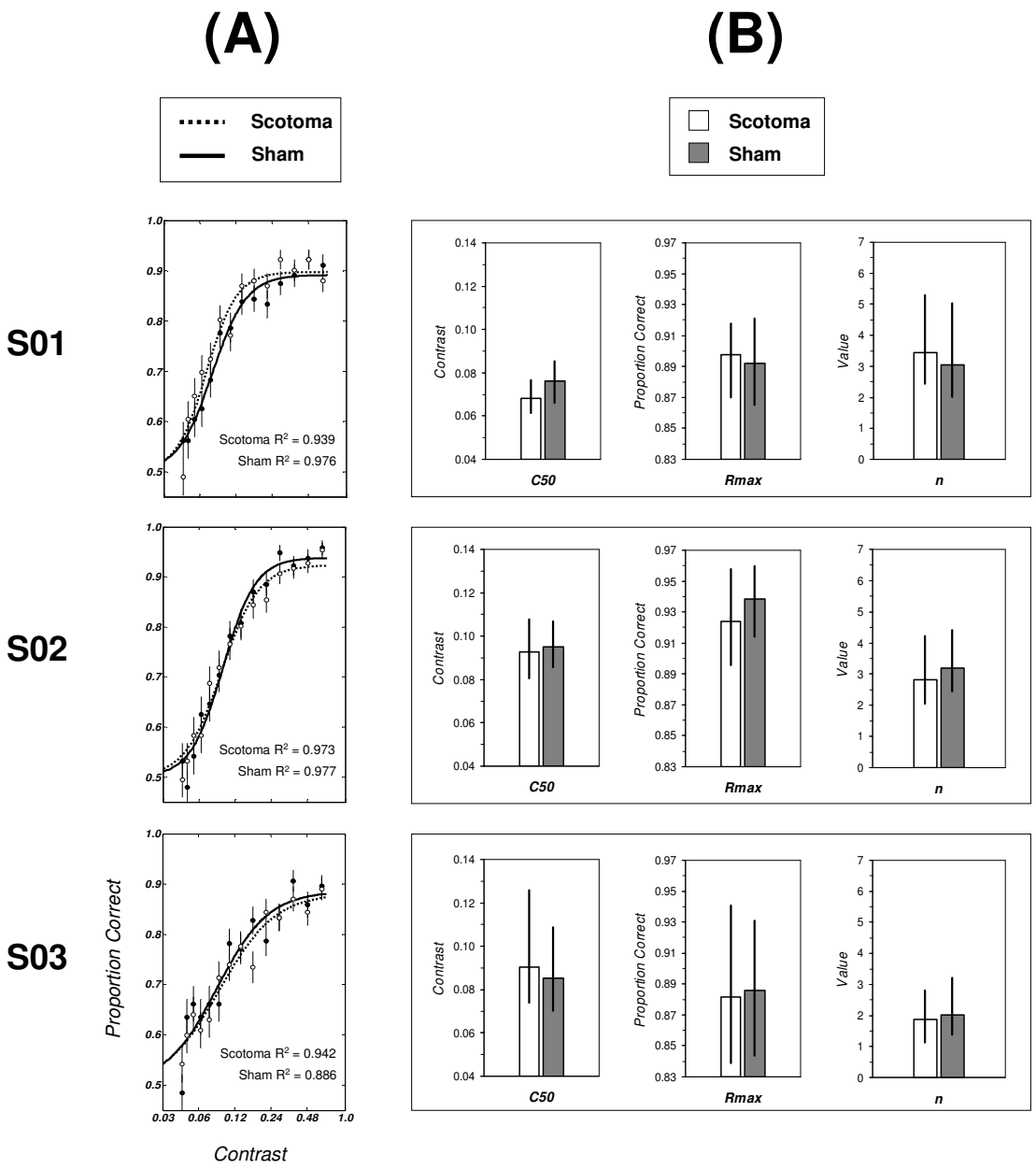

Figure 12. Contrast response functions and parameter bootstrapping from Experiment 3. (A) Fits to the Naka-Rushton equation for each psychophysical observer. R^2 values are given for fits to the two conditions (Scotoma and Sham). Error bars denote ±1 SD for the 10,000 bootstrap samples. Contrast level is plotted on a logarithmic scale. (B) parameter estimation and bootstrapped 95% confidence intervals for the three parameters of interest. No significant parameter differences were present for any of the three observers.

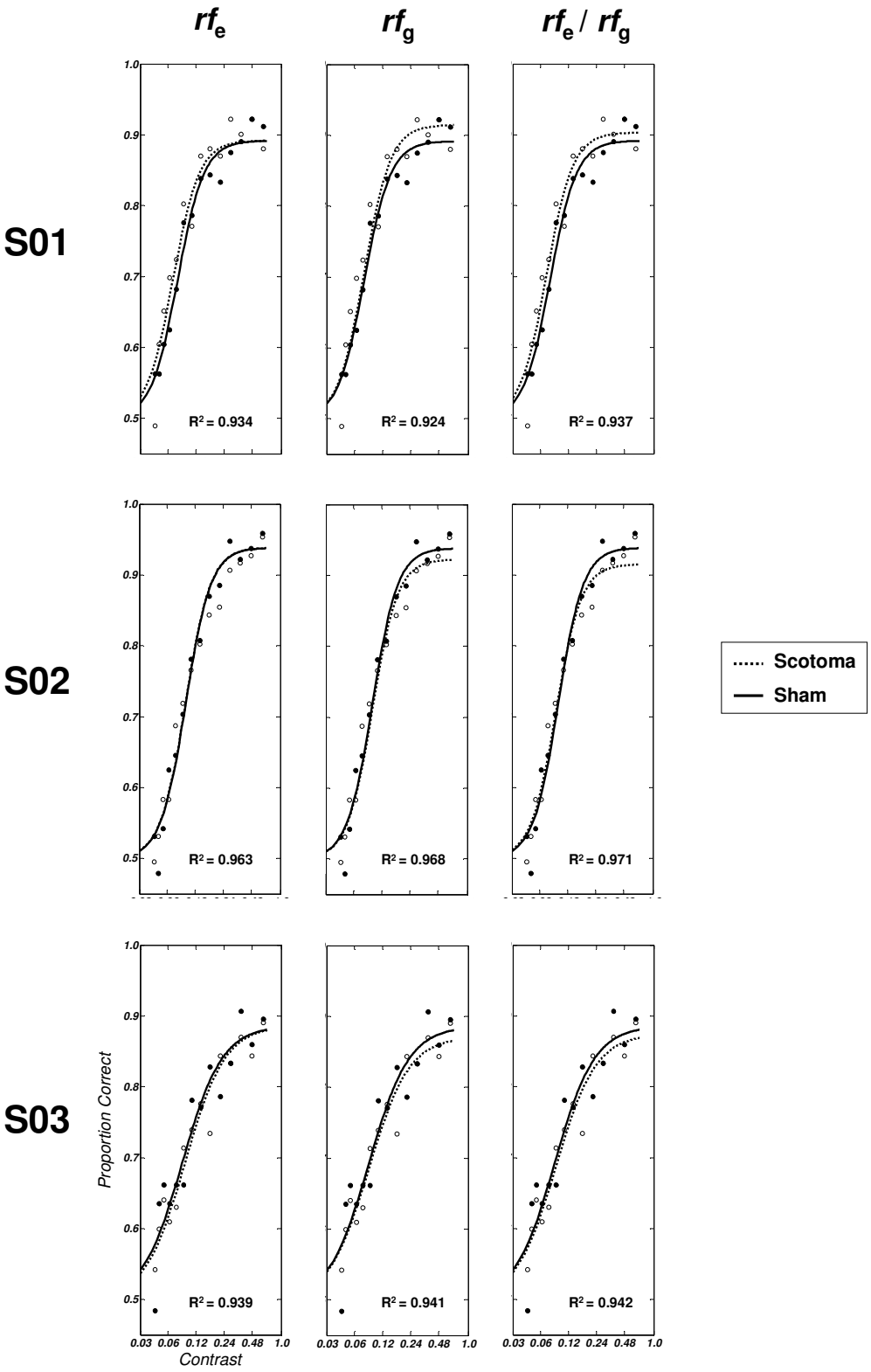

Figure 13. Fits of the three quantitative models in Experiment 3. R^2 values for the fit of each model are given within their respective panels. Contrast is plotted on a logarithmic scale. Winning models are not indicated as no model was clearly superior to the others.

Discussion

The IZ provides a source of input to TDZ by connecting it, via horizontal projections, with cortical areas that continue to receive visual input. That is, IZ provides invading activity into the TDZ. Experiment 3 examined changes in the neural representation of extra-scotoma space due to invading activity from IZ by measuring contrast response functions following a period of conditioning with an artificial scotoma.

No perceptual differences were found between Scotoma and Sham conditions for any observer. Neither bootstrapping nor quantitative model fits revealed any patterns or trends between Scotoma and Sham conditions. These results suggest that invading activity into the TDZ had no measurable effects of perceptual enhancement or distortion for extra-scotoma space at least in terms of the contrast response function. This suggests that activity-dependent disinhibition within the TDZ does not affect the receptive field dynamics of normal surrounding cortex (IZ). It could be the case that invading activity has no bearing on contrast response functions but would have perceptual consequences measurable through different dimensions (e.g., acuity, spatial frequency, etc.). Long-term changes in the representation of extra-scotoma space have been demonstrated in patients exhibiting long-term reorganization (Dilks et al., 2007) and it may be the case that measurable perceptual effects from extra-scotoma space are only measurable following extensive periods of cortical reorganization.

The null effects of Experiment 3 serve a secondary purpose in that they provide an additional control for the findings of Experiment 1. Experiment 1 and 3 differed only in the class of visual probe used and the range of contrasts tested. All other stimulus parameters were identical between the two studies. As such, the results of Experiment 1

are strengthened in that no argument can be made that experimental effects were due to some extraneous variable or idiosyncratic difference between Scotoma and Sham conditions.

CHAPTER 5

EXPERIMENT 4

Experiment 4 investigated the neural correlates of invading activity from IZ into TDZ using event-related potentials. VEPs were elicited from extra-scotoma space and thus represented activity arising from IZ. Early sensory components of the VEP (C1, P1, and N1) were assessed for amplitude modulations indicative of invading activity.

Method

Subjects

Fifteen naïve subjects (8 females) were recruited from the Georgia Institute of Technology undergraduate population. Subjects ranged in age from 18 to 21 (M=19.5, SD=1.1). All subjects reported normal or corrected to normal vision.

Stimuli and Procedure

Stimuli and procedure were identical to that of Experiment 2 with the exception that the visual probes used to elicit VEPs were extra-scotoma Gabor annuli maintained at a contrast of 0.80.

Electroencephalography

Electrophysiological recording adhered to the procedures and analyses described in Experiment 2.

Data Analysis

Data analysis was identical to that of Experiment 2 with the exception of the time windows of component analysis. Experiment 4 time windows were 90-135 ms for C1, 120-160 ms for P1, and 180-215 ms for N1. These time windows were defined according to the same procedures described in Experiment 2.

As in Experiment 2, an early negativity was present and overlapped with the C1 component. The same baseline correction procedure from Experiment 2 was used to visualize C1 scalp topographies. However, a period of 60-80 ms was used to perform the correction in Experiment 4.

Results

Behavioral Data

Accuracy in the discrimination of the tilt of extra-scotoma Gabor annuli was compared between Scotoma and Sham conditions through a paired-samples t-test. There was no significant difference in performance between Scotoma (M=0.869, SD=0.078) and Sham (M=0.884, SD=0.062) conditions, $t(14)=-1.39$, $p>.18$.

C1 Component

Resultant C1 scalp topographies and waveforms are displayed in Figure 14. Scalp distributions and polarity reversal between upper and lower visual fields are confirmative of the selective time range (90-135 ms) as the C1 component. Tests of C_{diff} against zero at electrodes CP1/2, P3/4, PO3/4, and Pz revealed no significant differences, $t(14)=.017$, $p>.98$, $t(14)=1.04$, $p>.31$, $t(14)=1.32$, $p>.20$, and $t(14)=.814$, $p>.42$, respectively. These

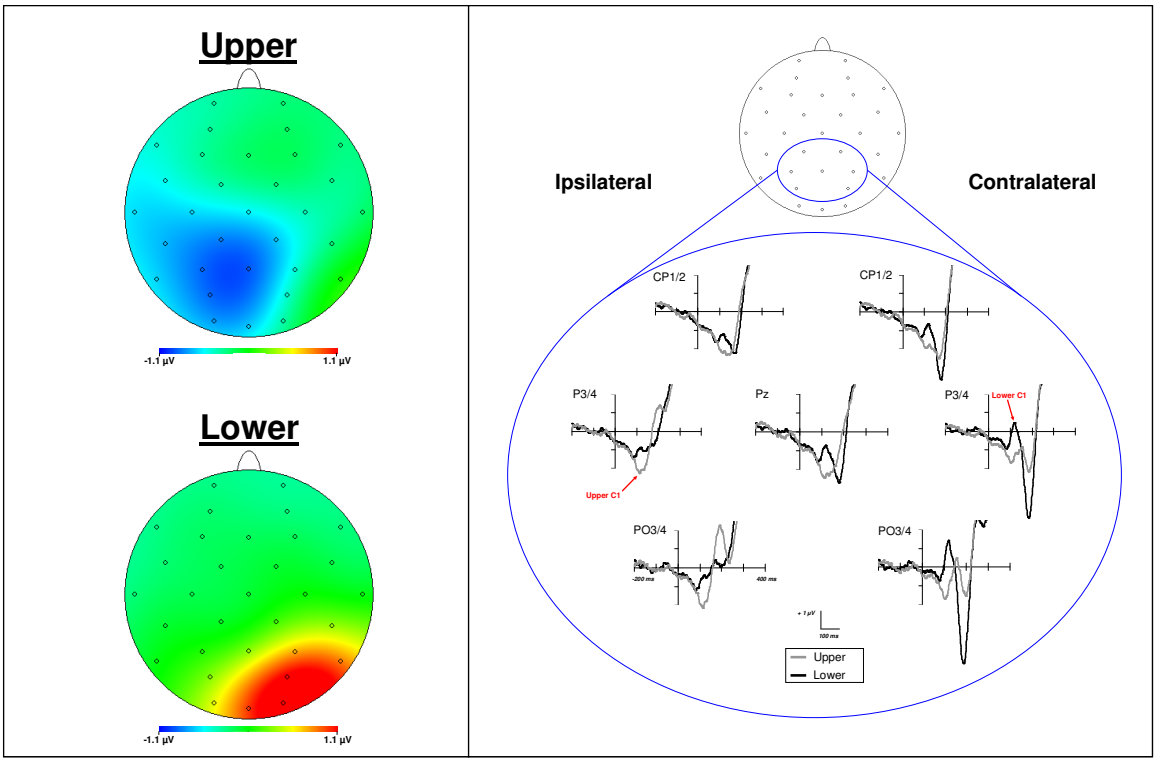

Figure 14. The C1 component from Experiment 4. Grand average scalp distributions of the C1 component (90 – 135 ms) are collapsed across left and right visual fields (left panel). Scalp distributions are arbitrarily mapped so that ipsilateral electrode positions are represented on the left and contralateral on the right. Grand average waveforms for upper and lower fields are shown in the right panel. The upper versus lower field polarity reversal along with the shift in scalp distribution clearly indicate the presence of C1 component.

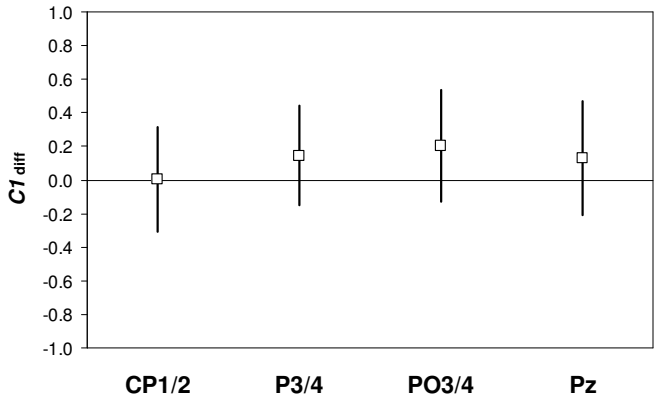

Figure 15. $C1_{diff}$ values for the four electrodes of analysis in Experiment 4. $C1_{diff}$ did not differ significantly from zero at any electrode, indicating no change in C1 between Scotoma and Sham conditions.

results indicate that there were no differences in C1 amplitude between Scotoma and Sham conditions. $C1_{diff}$ values for each electrode tested are plotted in Figure 15.

P1 Component

No differences in P1 amplitude were present at either O1/2, $t(14)=-1.50$, $p>.15$, or P7/8, $t(14)=-1.36$, $p>.19$. P1 scalp topographies and waveform plots of Scotoma and Sham conditions are pictured in Figure 16.

N1 Component

N1 amplitude was significantly greater in the Scotoma condition relative to the Sham condition at contralateral electrode O1/2, $t(14)=-2.21$, $p<.05$. No difference was found at contralateral P7/8, $t(14)=-1.75$, $p>.10$. N1 scalp maps and amplitude enhancement is depicted in Figure 16.

Discussion

Experiment 4 investigated the neural correlates of invading activity from IZ into TDZ by measuring VEPs elicited from extra-scotoma space. Analysis of C1, P1, and N1 amplitudes found no differences in C1 or P1 components between Scotoma and Sham conditions but revealed a significant modulation of N1 amplitude in the Scotoma condition. This modulation was such that the N1 elicited from extra-scotoma space was larger in the Scotoma than the Sham condition. N1 amplification is consistent with a neural correlate of invading activity. Invading activity from IZ into TDZ has a result of effectively increasing the neural representation of extra-scotoma space. Amplitude

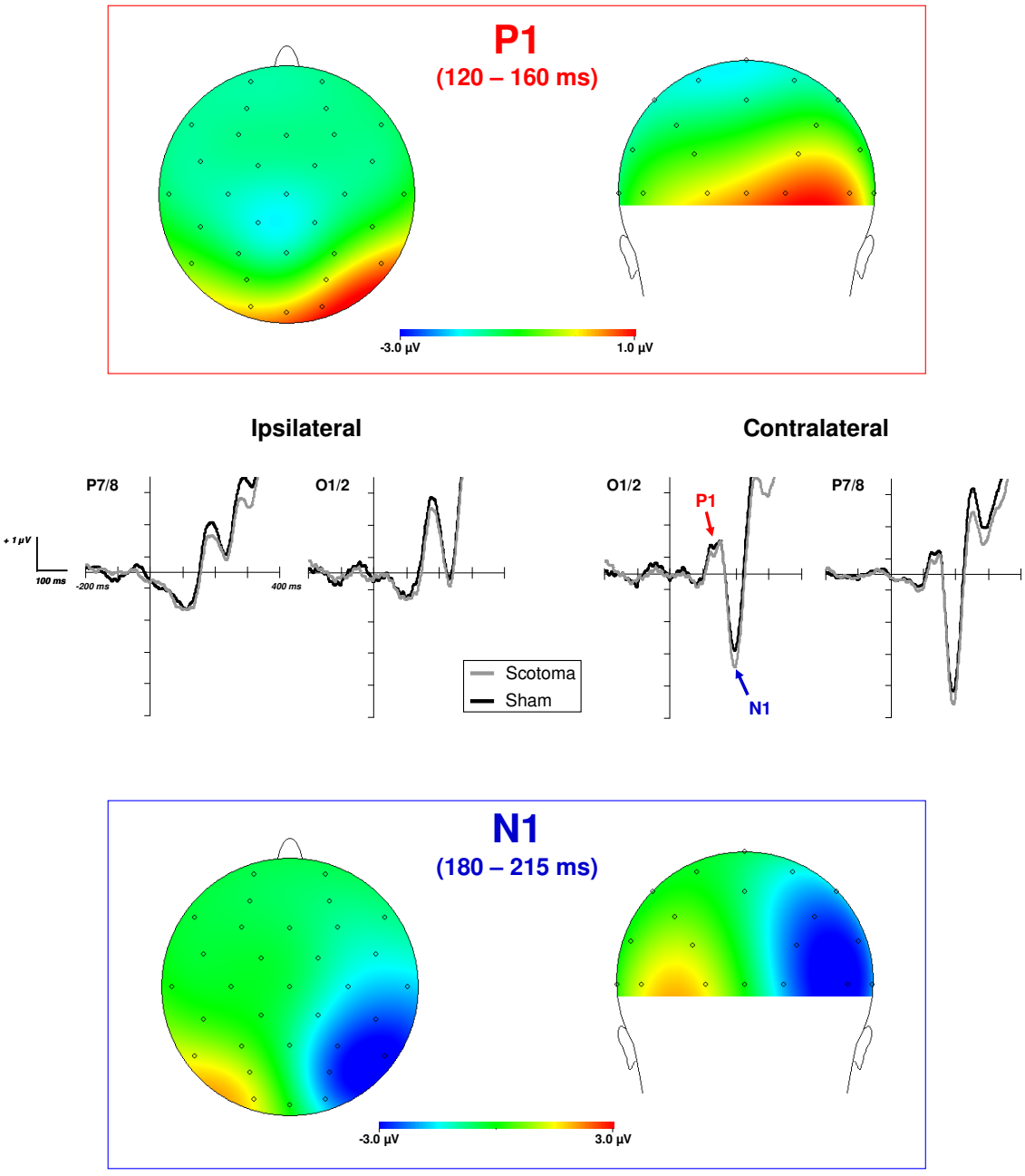

Figure 16. P1 and N1 components from Experiment 4. Grand average scalp topographies of P1 and N1 components are shown in the top and bottom panels, respectively. Waveforms are collapsed across visual quadrants. Scalp distributions are arbitrarily mapped such that ipsilateral electrode positions are represented on the left and contralateral on the right. No significant differences were present for the contralateral but there was a significant amplitude amplification of the N1 at contralateral O1/2 (middle). This amplification was such that N1 amplitude was greater in the Scotoma condition relative to Sham.

amplification of N1 is consistent with an increased response within TDZ due to invading activity.

Experiment 3 examined the perceptual consequences of invading activity from IZ but found no measurable differences between Scotoma and Sham conditions. However, the complementary ERP study found clear modulation of visuocortical activity consistent with invading activity. The discrepancy between the perceptual and neurophysiological investigation may be resolved by considering the nature of the invading zone of cortex. IZ continues to receive normal visual input and local inhibitory drive remains unchanged. In effect, activity within IZ itself should remain unaltered. That is, IZ provides the same perceptual-level information regardless of how TDZ changes. Though there is no alteration of visual processing within IZ, disinhibition within TDZ increases the efficacy of inputs from IZ into TDZ resulting in a measurable difference in neural response. Thus, the short-term effects of invading activity may only be measurable (perceptually) within the scotoma itself since IZ continues to respond normally despite the fact that a neural correlate of the activity can be measured from extra-scotoma space.

A neural correlate of invading activity was only apparent in the later N1 component, a result which suggests that invading activity occurred at a later stage of extrastriate visual processing. No evidence of invading activity was apparent at the level of V1 (indexed by C1) or earlier in extrastriate processing (indexed by P1). This result suggests that invading activity does not occur until later in the stream of visual processing, beginning at a relatively high level of the visual hierarchy. It is not entirely clear why invading activity was only apparent at a later in the stream of visual processing as one would predict that invading activity should begin at the same stage as TDZ

plasticity. That is, the effects would be expected in C1 and P1 as well since such modulations were apparent from TDZ (Experiment 2). It is possible that there was simply a failure to statistically detect such an effect or that the early effects of invading activity are too small to detect at the level of the scalp. However, the findings of N1 amplification may indicate the involvement of higher-order feedback in the induction of plasticity at earlier levels of the visual hierarchy.

The involvement of feedback projections in representational plasticity remains an unexplored area in the plasticity literature and it is largely assumed that plasticity within a DZ or TDZ is a local phenomenon mediated by horizontal projections (Gilbert, 1998; Calford, 2002). However, higher-order visual areas send a mass of feedback projections to lower areas of the hierarchy and there is compelling evidence to suggest that receptive field properties can be significantly modulated by such feedback (for review see Angelucci & Bullier, 2003). There is a distinct possibility that feedback projections may modulate, perhaps even induce, short-term plasticity within earlier cortical areas. Though speculative, this later N1 reflect a later, extrastriate source of invading activity. More specifically, invading activity may originate from higher-order visual areas and feedback into earlier areas. Such feedback could either be the direct source of invading activity or could modulates (gate) local invading activity within an earlier visual area. Scalp-recorded potentials cannot differentiate between feed-forward and feedback activity so a feedback interpretation is based solely on the time course of the N1 correlate of invading activity. This proposal of invading activity originating within a higher-order visual area cannot be verified further given the current dataset. Systematic investigation of the role of feedback in topographic plasticity is required.

CHAPTER 6

GENERAL DISCUSSION

The current investigations were concerned with establishing the neural mechanisms and processes that underlie short-term plasticity in the human visual system following temporary sensory deafferentation. Four experiments were conducted to examine the changes in receptive-field dynamics that occur with the induction of short-term plasticity by an artificial scotoma. Experiments 1 and 2 examined the receptive field dynamics within deafferented cortex (TDZ) using a psychophysical technique and event-related potentials, respectively. Experiments 3 and 4 were exploratory investigations that sought perceptual and neural correlates of invading activity from the cortical area surrounding TDZ – the invading zone, or IZ.

A neural mechanism widely held to be responsible for the effects of short-term plasticity is that of disinhibition wherein the TDZ is released from local GABAergic inhibition. Some have argued that the result of this disinhibition is an expansion of receptive fields through the unmasking of long-range horizontal connections (Das & Gilbert, 1995b; Pettet & Gilbert, 1992). Another proposal has suggested that the unmasking of these horizontal connections through disinhibition has the effect of increasing the neural response gain of TDZ neurons rather than expanding their receptive fields (DeAngelis et al., 1995). Both proposals have empirical support but neither fully considers the implications of disinhibition to neural processing and representations within TDZ.

I have proposed that the result of disinhibition on receptive field properties within TDZ is best described in terms of two separable but dependent processes. One is a process of receptive field expansion that occurs as a result of the unmasking of long-rang horizontal projections. The second process is one termed unrestricted gain where a reduction in inhibitory drive causes a loss of neural response selectivity. According to unrestricted gain, cells within the TDZ become more responsive overall but lose the specificity of their response. Unrestricted gain implies an overall increase in neural response but a reduction in signal-to-noise ratio due to the loss of selectivity.

The aforementioned processes of disinhibition were evaluated in Experiment 1 by measuring contrast response functions from within an artificial scotoma. In support of the two-process model of disinhibition contrast response functions exhibited enhanced perceptual thresholds but reduced asymptotic performance. Improved perceptual thresholds are predicted by the increased representation of intra-scotoma space within the TDZ due to receptive field expansions whereas reductions in asymptotic performance are predicted as a result of the multiplicative effects of unrestricted gain.

The two-process model of disinhibition is advantageous because it is biologically plausible and is able to fully describe a host of empirical results. It accounts for the seemingly contradictory results of receptive field expansion and receptive field gain (Pettet & Gilbert, 1992; DeAngelis et al., 1995) and accounts for several discrepant psychophysical findings as well (Kapadia et al., 1994; Mihaylov et al., 2007).

Experiment 2 provided a neural correlate of disinhibition within the TDZ. Visual evoked potentials were elicited from within the boundaries of an artificial scotoma. Conditioning with an artificial scotoma induced amplifications of the C1 and P1

components of the visual evoked potential. These amplitude amplifications are consistent with the occurrence of disinhibition within the TDZ and provide a non-invasive neural correlate of the process. Results from Experiment 2 further indicate that the process of disinhibition occurs as early as primary visual cortex in humans (at least with an artificial scotoma).

Two exploratory investigations were concerned with how plasticity within the TDZ affected cortical processing in the IZ. The induction of plasticity within the TDZ unmasks horizontal inputs that arise from IZ. As such, this invading activity may be expected to affect the processing of information by IZ. Experiments 3 and 4 examined the perceptual and neural correlates of invading activity by probing extra-scotoma space. No perceptual effects were apparent in contrast response functions. However, an electrophysiological correlate of invading activity was apparent in the N1 component (180-215 ms). N1 activity was such that its amplitude was amplified in the presence of an artificial scotoma, a result consistent with the increased invading activity into the TDZ. The N1 component reflects visual processing within higher-level extrastriate areas suggesting that invading activity from the IZ into the TDZ did not occur until a relatively late stage of visual processing. Though extensive investigation is necessary, this finding may point to the involvement of top-down feedback in short-term plasticity and disinhibition. More specifically, this N1 amplification may reflect invading activity that originates at a later stage of visual processing and feeds back to earlier visual areas (e.g., V1). Such feedback may be the source of short-term invading activity or may act to modulate local disinhibition and invading activity within earlier visual areas.

The investigations presented here enhance the understanding of the neural mechanisms of short-term visual plasticity and extend findings to humans. A conceptual framework of the processes of disinhibition has been provided and can be used to better understand and predict the effects of short-term plasticity (Experiment 1). A neural correlate of short-term visual plasticity and disinhibition has also been demonstrated for the first time in humans (Experiment 2). Additionally, exploratory investigations of the neural representations extra-scotoma space have suggested that feedback from higher-level sensory areas may play a role in the induction or modulation of short-term plasticity and disinhibition (Experiment 4). Although the investigations here concentrate on disinhibition in the context of sensory representational plasticity, the mechanism appears to be a ubiquitous component of neocortical processing. Disinhibition has been implicated not only in the topographical reorganization of sensory and motor areas (Calford, 2002) but also in a variety of forms of learning and memory (Froemke, Merzenich, & Schreiner, 2007; Paulsen & Moser, 1998; Tremere et al., 2005). In a broader scope, the investigations of this dissertation are informative about general mechanisms of cortical processing and may have implications that extend well beyond the domain of visual cortical processing.

APPENDIX A: ASSESSMENT OF PRACTICE EFFECTS IN EXPERIMENT 1

Systematic differences practice effects between Scotoma and Sham conditions were assessed over the twelve experimental sessions. For each session, a difference score between mean accuracy in each condition was calculated (Sham accuracy – Scotoma accuracy) and submitted to a linear regression. No significant trends were present (Figure 17).

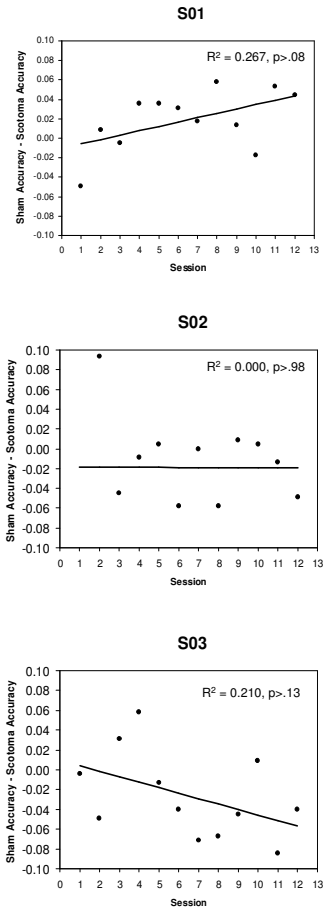

Figure 17. Differences in accuracy between Scotoma and Sham conditions as a function of experimental session.

REFERENCES

Albrecht, D.G. & Hamilton, D.B. (1982). Striate cortex of monkey and cat: contrast response function. *Journal of Neurophysiology, 48,* 217-237.

Angelucci, A. & Bullier, J. (2003). Reaching beyond the classical receptive field of V1 neurons: horizontal and feedback axons? *Journal of Physiology – Paris, 97,* 141-154.

Bach (1996). The Freiburg Visual Acuity test – automatic measurement of visual acuity. *Optometry & Vision Science, 73,* 49-53.

Baker, C.I., Peli, E., Knouf, N., & Kanwisher, N.G. (2005). Reorganization of visual processing in macular degeneration. *Journal of Neuroscience, 25,* 614-618.

Baker, C.I., Dilks, D.D., Peli, E., & Kanwisher, N. (2009). Reorganization of visual processing in macular degeneration: replication and clues about the role of foveal loss. *Vision Research, 48,* 1910-1919.

Benson, D.L., Huntsman, M.M., & Jones, E.G. (1994). Activity-dependent changes in GAD and preprotachykinin mRNAs in visual cortex of adult monkeys. *Cerebral Cortex, 4,* 40-51.

Blasdel, G.G. & Lund, J.S. (1983). Termination of afferent axons in macaque striate cortex. *Journal of Neuroscience, 3,* 1389-1413.

Calford, M.B. (2002). Dynamic representational plasticity in sensory cortex. *Neuroscience, 111,* 709-738.

Calford, M.B., Chino, Y.M., Das, A., Eysel, U.T., Gilbert, C.D., Heinen, S.J., Kaas, J.H., & Ullman, S. (2005). Neuroscience: rewiring the adult brain. *Nature, 438,* E3.
Calford, M.B., Schmid, L.M., and Rosa, M.G.P. (1999) Monocular focal retinal lesions induce short-term topographic plasticity in adult visual cortex. *Proceedings of the Royal Society of London Series B, 266,* 499-507.

Calford, M.B. & Tweedale, R. (1988). Immediate and chronic changes in responses of somatosensory cortex in adult flying-fox after digit amputation. *Nature, 332,* 446-448.

Calford, M.B. & Tweedale, R. (1991a). Acute changes in cutaneous receptive fields in primary somatosensory cortex after digit denervation in adult flying fox. *Journal of Neurophysiology, 65,* 178-187.

Calford, M.B. & Tweedale, R. (1991b). Immediate expansion of receptive fields of neurons in area 3b of macaque monkeys after digit denervation. *Somatosensory & Motor Research, 8,* 249-260.

Calford, M.B., Wang, C., Taglianetti, V., Waleszcyk, W.J., Burke, W., & Dreher, B. (2000). Plasticity in adult cat visual cortex (area 17) following circumscribed monocular lesions of all retinal layers. *Journal of Physiology, 524,* 587-602.

Calford, M.B., Wright, L.L., Metha, A.B., & Taglianetti, V. (2003). Topographic plasticity in primary visual cortex is mediated by local corticocortical connections. *Journal of Neuroscience, 23,* 6434-6442.

Carrasco, M. (2006). Covert attention increases contrast sensitivity: psychophysical, neurophysiological and neuroimaging studies. *Progress in Brain Research, 154,* 33-70.

Chapman, B. & Stone, L.S. (1996). Turning a blind eye to cortical receptive fields. *Neuron, 16,* 9-12.

Chino, Y.M., Kaas, J.H., Smith, E.L., Langston, A.L., & Cheng, H. (1992). Rapid reorganization of cortical maps in adult cats following restricted deafferentation in retina. *Vision Research, 32,* 789-796.

Clark, V.P., Fan, S., Hillyard, S.A. (1995). Identification of early visually evoked potential generators by retinotopic and topographic analysis. *Human Brain Mapping, 2,* 170-187.

Darian-Smith, C. & Gilbert, C.D. (1995). Topographic reorganization in the striate cortex of the adult cat and monkey is cortically mediated. *Journal of Neuroscience, 15,* 1631-1647.

Das, A. & Gilbert, C.D. (1995a). Long-range horizontal connections and their role in cortical reorganization revealed by optical recording of cat primary visual cortex. *Nature, 375,* 780-784.

Das, A. & Gilbert, C.D. (1995b). Receptive field expansion in adult visual cortex is linked to dynamic changes in strength of cortical connections. *Journal of Neurophysiology, 74,* 779-792.

DeAngelis, G.C, Akiyuki, A., Ohzawa, I., & Freeman, R.D. (1995). Receptive field structure in the visual cortex: Does selective stimulation induce plasticity. *Proceedings of the National Academy of Sciences United States of America, 92,* 9682-9686.

DeAngelis, G.C, Ohzawa, I., & Freeman, R.D. (1993). Spatiotemporal organization of simple-cell receptive fields in the cat's striate cortex. II. Linearity of temporal and spatial summation. *Journal of Neurophysiology, 69,* 1118–1135.

De Weerd, P. (2006). Perceptual filling-in: more than the eye can see. *Progress in Brain*

Research, 154, 227-243.

De Weerd, P., Desimone, R., & Ungerleider, L.G. (1998). Perceptual filling-in: a parametric study. *Vision Research, 38,* 2721-2734.

De Weerd, P., Gattass, R., Desimone, R. & Ungerleider, L.G. (1995). Responses of cells in monkey visual cortex during perceptual filling-in of an artificial scotoma. *Nature, 377,* 731-734.

De Weerd, P. & Pessoa, L. (2003). Filling-in: more than meets the eye. In: *Filling-in: From Perceptual Completion to Skill Learning*. Pessoa, L. & De Weerd, P. (Eds.). Oxford University Press.

De Weerd, P., Smith, E., & Greenberg, P. (2006). Effects of selective attention on perceptual filling-in. *Journal of Cognitive Neuroscience, 18,* 335-347.

Di Russo, F., Mantinez, A., Sereno, M.I., Pitzalis, S., & Hillyard, S.A. (2001). Cortical sources of the early components of the visual evoked potential. *Human Brain Mapping, 15,* 95-111.

Dilks, D.D., Serences, J.T., Rosenau, B.J., Yantis, S., & McCloskey, M. (2007). Human adult cortical reorganization and consequent visual distortion. *Journal of Neuroscience, 27,* 9585-9594.

Dilks, D.D., Baker, C.I., Peli, E., & Kanwisher, N. (2009). Reorganization of visual processing in macular degeneration is not specific to the "preferred retinal locus". *Journal of Neuroscience, 29,* 2768-2773.

Dougherty, R.F., Koch, V.M., Brewer, A.A., Fischer, B., Modersitzki, J., & Wandell, B.A. (2003). Visual field representations and locations of visual areas V1/2/3 in human visual cortex. *Journal of Vision, 3,* 586-598.

Dreher, B., Burke, W., & Calford, M.B. (2001). Cortical plasticity revealed by circumscribed retinal lesions or artificial scotomas. *Progress in Brain Research, 134,* 217-245.

Efron, B. & Tibshirani, R. (1993). *Introduction to the bootstrap.* New York: Chapmann & Hall.

Eysel, U.T. (1982). Functional reconnections without new axonal growth in a partially denervated visual relay nucleus. *Nature, 299,* 422-444.

Fitzpatrick, D. (2000). Seeing beyond the receptive field in primary visual cortex. *Current Opinion in Neurobiology, 10,* 438-443.

Froemke, R.C., Merzenich, M.M., & Schreiner, C.E. (2007). A synaptic memory trace

for cortical receptive field plasticity. *Nature, 450,* 425-429.

Gilbert, C.D. (1998). Adult cortical dynamics. *Physiological Review, 78,* 467-485.

Gilbert, C.D., Das, A., Ito, M., Kapadia, M., & Westheimer, G. (1996). Spatial integration and cortical dynamics. *Proceedings of the National Academy of Sciences United States of America, 93,* 615-622.

Gilbert, C.D. & Wiesel, T.N. (1992). Receptive field dynamics in adult primary visual cortex. *Nature, 356,* 150-152.

Heinen, S.J. & Skavenski, A.A. (1991). Recovery of visual responses in foveal V1 neurons following bilateral foveal lesions in adult monkey. *Experimental Brain Research, 83,* 670-674.

Hubel, D.H. & Wiesel, T.N. (1970). The period of susceptibility to the physiological effects of unilateral eye closure in kittens. *Journal of Physiology, 206,* 419-436.

Hubel, D.H. & Wiesel, T.N. (1974). Uniformity of monkey striate cortex: a parallel relationship between field size, scatter, and magnification factor. *Journal of Comparative Neurology, 158,* 295-305.

Jeffreys, D.A., & Axford, J.G. (1972a). Source locations of pattern-specific components of human visual evoked potentials. I. Component of striate cortical origin. *Experimental Brain Research, 16,* 1-21.

Jeffreys, D.A., & Axford, J.G. (1972b). Source locations of pattern-specific components of human visual evoked potentials. II. Component of extrastriate cortical origin. *Experimental Brain Research, 16,* 22-40.

Jones, E.G. (1990). The role of afferent activity in the maintenance of primate neocortical function. *Journal of Experimental Biology, 153,* 155-176.

Kaas, J.H., Krubitzer, L.A., Chino, Y.M., Langston, A.L., Polley, E.H., & Blair, N. (1990). Reorganization of retinotopic cortical maps in adult mammals after lesions of the retina. *Science, 248,* 229-231.

Kapadia, M.K., Gilbert, C.D., & Westheimer, G. (1994). A quantitative measure for short-term cortical plasticity in human vision. *Journal of Neuroscience, 14,* 451-457.

Ling, S. & Carrasco, M. (2006). Sustained and transient covert attention enhance the signal via different contrast response functions. *Vision Research, 46,* 1210-1220.

Lu, Z.L. & Dosher, B.A. (1998). External noise distinguishes attention mechanisms. *Vision Research, 38,* 1183-1198.

Lu, Z.L., & Dosher, B.A. (1999). Characterizing human perceptual inefficiencies with equivalent internal noise. *Journal of the Optical Society of America, 16,* 764-778.

Martinez, A., Anllo-Vento, L., Sereno, M.I., Frank, L.R., Buxton, R.B., Dubowitz, D.J., Wong, E.C., Hinrichs, H., Heinze, H.J., Hillyard, S.A. (1999). Involvement of striate and extrastriate visual cortical areas in spatial attention. *Nature Neuroscience, 2,* 364-369.

Martinez, A., Di Russo, F., Anllo-Vento, L., Sereno, M.I., Buxton, R.B., & Hillyard, S.A. (2001a). Putting spatial attention on the map: timing and localization of stimulus selection processes in striate and extrastriate visual areas. *Vision Research, 41,* 1437-1457.

Martinez, A., Di Russo, F., Anllo-Vento, & Hillyard, S.A. (2001b). Electrophysiological analysis of cortical mechanisms of selective attention to high and low spatial frequencies. *Clinical Neurophysiology, 112,* 1980-1998.

Masuda, Y., Dumoulin, S.O., Nakadomari, S., & Wandell, B.A. (2008). V1 projection zone signals in human macular degeneration depend on task, not stimulus. *Cerebral Cortex, 18,* 2483-2493.

McGuire, B.A., Gilbert, C.D., Rivlin, P.K., & Wiesel, T.N. (1991). Targets of horizontal connections in macaque primary visual cortex. *Journal of Comparative Neurology, 305,* 370-392.

Merzenich, M.M., Kaas, J.H., Wall, J., Nelson, R.J., Sur, M., & Felleman, D. (1983a). Topographic reorganization of somatosensory cortical areas 3b and 1 in adult monkeys following restricted deafferentation. *Neuroscience, 8,* 33-55.

Merzenich, M.M., Kaas, J.H., Wall, J., Sur, M., Nelson, R.J., & Felleman, D. (1983b). Progression of change following median nerve section in the cortical representation of the hand in areas 3b and 1 in adult owl and squirrel monkeys. *Neuroscience, 10,* 639-665.

Merzenich, M.M., Nelson, R.J., Stryker, M.P., Cynader, M.S., Schoppmann, A. Zook, J.M. (1984). Somatosensory cortical map changes following digit amputation in adult monkeys. *Journal of Comparative Neurology, 224,* 591-605.

Mihaylov, P., Manahilov, V. Simpson, W.A., & Strang, N.C. (2007). Induced internal noise in perceptual artificial scotomas created by surrounding dynamic noise. *Vision Research, 47,* 1479-1489.

Morgan, C.M. & Shatz, H. (1985). Idiopathic macular holes. *American Journal of Opthalmology, 99,* 437-444.

Paulsen, O., & Moser, E.I. (1998). A model of hippocampal memory encoding and retrieval: GABAergic control of synaptic plasticity. *Trends in Neurosciences, 21,* 273-278.

Pettet, M.W., & Gilbert, C.D. (1992). Dynamic changes in receptive-field size in cat primary visual cortex. *Proceedings of the National Academy of Sciences United States of America, 89,* 8366-8370.

Rajan, R., Irvine, D.R.F., Wise, L.Z., & Heil, P. (1993). Effect of unilateral partial cochlear lesions in adult cats on the representation of lesioned and unlesioned cochleas in primary auditory cortex. *Journal of Computational Neurology, 338,* 17-49.

Ramachandran, V.S. & Gregory, R.L. (1991). Perceptual filling in of artificially induced scotomas in human vision. *Nature, 350,* 699-702.

Reale, R.A. & Imig, T.J. (1980). Tonotopic organization in auditory cortex of the cat. *Journal of Comparative Neurology, 192,* 265-291.

Rozier, A.M., Arckens, L., Demeulemeester, H., Orban, G.A., Eysel, U.T., Wu, Y.J., Vandesande, F. (1995). Effect of sensory deafferentation on immunoreactivity of GABAergic cells and on GABA receptors in the adult cat visual cortex. *Journal of Comparative Neurology, 359,* 476-489.

Rasmusson (1982). Reorganization of raccoon somatosensory cortex following removal of the fifth digit. *Journal of Comparative Neurology, 205,* 313-326.

Robertson, D. & Irvine D.R.F. (1989). Plasticity of frequency organization in auditory cortex of guinea pigs with partial unilateral deafness. *Journal of Computational Neurology, 282,* 456-471.

Rosier, A.M., Arckens, L., Demeulemeester, H., Orban, G.A., Eysel, U.T., Wu, Y.J., & Vandelsande, F. (1995). Effect of sensory deaffertation on immunoreactivity of GABAergic cells and on GABA receptors in the adult cat visual cortex. *Journal of Comparative Neurology, 359,* 476-489.

Sanes, J.N., Suner, S., & Donoghue, J.P. (1990). Dynamic organization of primary motor cortex output to target muscles in adult rats. I. Long-term patterns of reorganization following motor or mixed peripheral nerve lesions. *Experimental Brain Research, 79,* 479-491.

Schmid, L.M., Rosa, M.G.P., & Calford, M.B. (1995). Retinal-detachment induces massive immediate reorganization in visual cortex. *NeuroReport, 65,* 1349-1353.

Schmid, L.M., Rosa, M.G.P., Calford, M.B., & Ambler, J.S. (1996). Visuotopic

reorganization in the primary visual cortex of adult cats following monocular and binocular retinal lesions. *Cerebral Cortex, 6,* 388-405.

Schumacher, E.H., Jacko, J.H., Primo, S.A., Main, K.L., Moloney, K.P., Kinzel, E.N., & Ginn, J. (2008). Reorganization of visual processing is related to eccentric viewing in patients with macular degeneration. *Restorative Neurology & Neuroscience, 26,* 391-402.

Sclar G., Maunsell, J.H., & Lennie, P. (1990). Coding of image contrast in central visual pathways of the macaque monkey. *Vision Research, 30,* 1-10.

Sceniak, M.P., Ringach, D.L., Hawken, M.J., & Shapley, R. (1999). Contrast's effect on spatial summation by macaque V1 neurons. *Nature Neuroscience, 2,* 733-739.

Sillito, A.M. (1975). The contribution of inhibitory mechanisms to the receptive field properties of neurons in the striate cortex of the cat. *Journal of Physiology, 250,* 305-329.

Smith, R.G., Lea, S.J.H., & Galloway, N.R. (1990). Visual performance in idiopathic macular holes. *Eye, 4,* 190-194.

Smirnakis, S.M., Brewer, A.A., Schmid, M.C., Tolias, A.S., Schüz, A., Augath, M., Inhoffen, W., Wandell, B.A., & Logothetis, N.K. (2005). Lack of long-term cortical reorganization after macaque retinal lesions. *Nature, 435,* 300-307.

Sunness, J.S., Liu, T., & Yantis, S. (2004). Retinotopic mapping of the visual cortex using functional magnetic resonance imaging in a patient with central scotomas from atrophic macular degeneration. *Opthalmaology, 111,* 1595-1598.

Tootell, R.B.H., Switkes, E., Silverman, M.S. & Hamilton, S.L. (1988). Functional anatomy of macaque striate cortex. II: Retinotopic organization. *Journal of Neuroscience, 8,* 1531-1568.

Tremere, L.A., De Weerd, P., & Pinaud, R. (2003). Contributions of inhibitory mechanisms to perceptual completion and cortical reorganization. In: *Filling-in: From Perceptual Completion to Cortical Reorganization.* Pessoa, L. & De Weerd (Eds.), Oxford University Press.

Tremere, L.A., De Weerd, P., & Pinaud, R. (2005). A Unified Theoretical Framework for Plasticity in Visual Circuitry. In: *Plasticity in the Visual System: From Genes to Circuits.* Pinaud, R., Tremere, L.A., & De Weerd, P. (Eds.), Springer-Verlag, New York. Chapter 16, pp 347-355.

Treue, S. (2001). Neural correlates of attention in primate visual cortex. *Trends in Neurosciences, 24,* 295-300.

Tusa, R.J., Palmer, L.A., & Rosenquist, A.C. (1978). The retinotopic organization of area 17 (striate cortex) in the cat. *Journal of Comparative Neurology, 177,* 213-235.

Volchan, E. & Gilbert, C.D. (1995). Interocular transfer of receptive field expansion in cat visual cortex. *Vision Research, 35,* 1-6.

Wichmann, F.A. & Hill, N.J. (2001a). The psychometric function: I. Fitting, sampling, and goodness of fit. *Perception & Psychophysics, 63,* 1293-1313.

Wichmann, F.A. & Hill, N.J. (2001b). The psychometric function: II. Bootstrap-based confidence intervals and sampling. *Perception & Psychophysics, 63,* 1314-1329.

Wolf, W., Hicks, T.P., & Albus, K. (1986). The contribution of GABA-mediated inhibitory mechanisms to visual response properties of neurons in the kitten's striate cortex. *Journal of Neuroscience, 6,* 2779-2795.

Zur, D. & Ullman, S. (2003). Filling-in of retinal scotomas. *Vision Research, 43,* 971-982.